Molecular Phylogenetics and Evolution 130 (2019) 244–258

Contents lists available at ScienceDirect

Molecular Phylogenetics and Evolution

journal homepage: www.elsevier.com/locate/ympev

Diversification and historical demography of the rapid racerunner (*Eremias velox*) in relation to geological history and Pleistocene climatic oscillations in arid Central Asia

Jinlong Liu[a,b], Xianguang Guo[a,*], Dali Chen[c], Jun Li[d], Bisong Yue[b], Xiaomao Zeng[a,*]

[a] Chengdu Institute of Biology, Chinese Academy of Sciences, Chengdu 610041, China
[b] Key Laboratory of Bio-resources and Eco-environment of Ministry of Education, College of Life Sciences, Sichuan University, Chengdu 610065, China
[c] Department of Parasitology, West China School of Basic Medical Sciences and Forensic Medicine, Sichuan University, Chengdu 610041, China
[d] College of Life Science and Technology, Xinjiang University, Urumqi 830046, China

ARTICLE INFO

Keywords:
Aridification
Ecological niche modeling
Eremias
Last glacial maximum
Phylogeography
Pleistocene climatic oscillations

ABSTRACT

Late Cenozoic stepwise aridification has transformed Central Asia into an arid environment, and the Pleistocene climatic oscillations exerted further ecological impact. Therefore, both aridification and glaciation would have considerably influenced the evolution of many midlatitude species in arid Central Asia (ACA). However, strong biotic evidence supporting this role is still lacking. Here, we test this perspective using a phylogeographic study of *Eremias velox*, which is an arid-adapted lizard, across ACA using sequences from mitochondrial cytochrome *b* and 12S rRNA genes. Phylogenetic analyses of the concatenated data, including 595 specimens from 107 localities, revealed ten geographically correlated lineages that diverged by 1.1–15.4% for the cytochrome *b* gene and 1.0–10.3% for the 12S rRNA gene, which were estimated to have coalesced ~6.23 million years ago. Ancestral area estimations suggested that *E. velox* originated from the Iranian Plateau and then dispersed into Central Asia. The intensification of aridification across Central Asia during the Late Pliocene may have facilitated the rapid radiation of this arid-adapted lizard throughout this vast territory. Subsequently, the geological events (e.g., uplift of the Kopet-Dagh, Tianshan and Greater Caucasus Mountains) and glacial oscillations during the Pleistocene triggered the progressive diversification of *E. velox*. The most recent common ancestor of the Caucasus-Central Asia clade was dated to approximately 2.05 Ma. Specifically, the diversification between the Caucasus clade (VI, VII) and the Central Asia clade (VIII, IX, X), and within the Central Asia clade may have been established and partially maintained by repeated transgressions of the Caspian Sea during the Pleistocene and Holocene. In contrast to demographic and/or range contractions in response to climatic changes during the Last Glacial Maximum (LGM) of the populations (Clades VI and X) from the Caucasus-Central Asia clade, mitochondrial evidence and ecological niche modeling support the signature of demographic and range expansions during the LGM for the Clade V populations (*E. v. roborowskii*, being endemic to the Turpan Depression). The effect of Pleistocene climatic changes on the historical demography of this arid-adapted species may be lineage-specific, depending predominantly on animal physiology and geography. Finally, we discuss the taxonomic implications, such as the appearance of the Turkmenistan populations as a distinct species, and *E. v. roborowskii* deserving a full species status.

1. Introduction

Geological events and climate fluctuations have played key roles in shaping the current patterns of genetic diversity on Earth (Hewitt, 2000, 2004). Spatial or temporal environmental heterogeneity is one of the major drivers of population divergence (Wang and Bradburd, 2014) and ultimately species diversification (Coyne and Orr, 2004; Tews et al., 2004). Consequently, a positive association between habitat discontinuity (e.g., the occurrence of physical barriers) and intraspecific diversity (genetic structure and/or structured lineage distribution) is expected (Avise, 2000). In the same context, historically stable habitats, which allow populations to remain in place over time, are positively correlated with high levels of intrapopulation genetic variability and demographic equilibrium (Carnavalet al., 2009). The

* Corresponding authors.
E-mail addresses: guoxg@cib.ac.cn (X. Guo), zengxm@cib.ac.cn (X. Zeng).

https://doi.org/10.1016/j.ympev.2018.10.029
Received 1 February 2018; Received in revised form 21 October 2018; Accepted 22 October 2018
Available online 26 October 2018
1055-7903/

opposite situation is expected for areas that have been repeatedly exposed to Pleistocene climatic oscillations, during which populations exhibit signatures of demographic decline or growth, depending largely on the adaptation of organisms (e.g., environmental tolerance and dispersal ability) (Avise, 2012).

One example of a dynamic and heterogeneous scenario is arid Central Asia (also called the arid Asian interior, ACA, in this paper), which accounts for one-third of the arid regions in the world, and the processes of aridification and Pleistocene glaciation cycles would have had important evolutionary consequences for the biota in this area (e.g., Jia et al., 2012; Melville et al., 2009; Shi et al., 2013). Arid Central Asia ranges from approximately 35–53°N, stretching from the Caspian Sea to the western border of China. This region covers the five post-Soviet Central Asian countries, northern Iran and Afghanistan, northwest China, and the southern Mongolian Plateau. Late Cenozoic stepwise aridification in Central Asia is thought to be one of the most prominent climate changes in the Northern Hemisphere (An et al., 2001; Guo et al., 2002; Sun et al., 2010). Aridification of the ACA has generally been linked to the Tibetan Plateau uplift (Guo et al., 2008), Paratethys shrinkage (Bosboom et al., 2011; Zhang et al., 2007) and global cooling (Lu et al., 2010; Miao et al., 2012; Tang et al., 2011). At present, ACA is characterized by multiple landscapes, including mountains, valleys and desert basins. Arid Central Asia also harbors one of the world's biodiversity hotspots, i.e., the Mountains of Central Asia (Myers et al., 2000), suggesting a complex evolutionary history of the local biota in this region. However, the ecological and evolutionary consequences of the Late Cenozoic stepwise aridification in Central Asia have been much less examined from a phylogeographic perspective (Garcia-Porta et al., 2012; Shi et al., 2013). In fact, the phylogeography of the world's arid regions has been studied very little in general (Byrne et al., 2008).

Global cooling during the Pleistocene glacial maxima (GM) imposed a further significant impact on the evolution of biodiversity (Hewitt, 2000). The Last Glacial Maximum (LGM; 0.026–0.019 Ma) (Clark et al., 2009) was an important climatic event characterized by low temperatures and precipitation in comparison to the current climate. The ranges of temperate-adapted taxa are generally inferred to have contracted during the LGM, as ice cover and unsuitably cold and dry climates forced species into glacial refugia, from which they subsequently expanded as the climate warmed (Hewitt, 2004; Provan and Bennett, 2008). Despite the historical focus on locating glacial refugia, it has become apparent that this model of GM contraction is not universally applicable to biota from unglaciated regions or cold-adapted taxa in the Northern Hemisphere (Galbreath et al., 2009; review by Kearns et al., 2014), even to systems for which it might typically be assumed. For example, the arid-adapted Grey Butcherbird (*Cracticus torquatus*) in Australia was shown to fit a model of GM expansion (Kearns et al., 2014), which is contrary to the common assumption of contraction to refugia. In addition, two recent studies of the temperate salamander species *Plethodon serratus* and steppe and meadow vipers (*Vipera ursinii* and *Vipera renardi*), rejected the universal applicability of the GM contraction model to temperate taxa and reiterated the importance of considering the natural history of individual species (Newman and Austin, 2015; Zinenko et al., 2015). Given that the GM largely resulted in the expansion of arid zones in ACA, at least in northwest China (Fang et al., 2002; Lu et al., 2013; Yang et al., 2006), it could be expected that arid-adapted species might have undergone demographic and range expansion at the GM. Under the GM expansion model, range restrictions and isolation might have occurred only during the short interglacial times; thus, low genetic structuring should be expected between populations of arid-adapted species due to the short time spent in isolation. Examples are accumulating in the northwest China area of ACA, lending some preliminary support to this idea (Cheng et al., 2017; Lv et al., 2016; Wang et al., 2013). As such, widespread arid-adapted species constitute a promising system to assess the joint effects of geographic complexity and glacial cycles on intraspecific population differentiation and population dynamics.

The rapid racerunner, *Eremias velox* Pallas, 1771 belongs to the Eurasian genus *Eremias* and is one of the most taxonomically complex taxa within the Lacertidae family (Guo et al., 2011). As one of the most typical and widespread desert lizards within ACA, *E. velox* occurs in a variety of habitats from sand dunes and gravel deserts to plateau mountains (Szczerbak, 1974, 1975, 2003; Zhao et al., 1999). This lizard also has limited dispersal ability (Wang and Autumn, 1990). Thus, the arid-adapted species *E. velox* can serve as an excellent model for investigating how geography and past climate changes affected the evolution of biodiversity in ACA. However, morphology-based taxonomy or molecular-based phylogeny techniques have previously failed to congruently recognize the intra- or even interspecific differentiations of this lizard. It is now widely recognized that *E. velox* constitutes a complex assembly of more or less well separated populations and subspecies. Traditionally, based on morphological traits, four geographically distinct populations were allocated subspecies statuses (Eremchenko and Panfilov, 1999; Szczerbak, 1974, 1975, 2003). Several recent molecular phylogenetic studies (Liu et al., 2014; Rastegar-Pouyani, 2009; Rastegar-Pouyani et al., 2012), using either mitochondrial markers (cytochrome *b* and 12S rRNA) or ISSR-PCR fingerprints, have identified seven geographically distinct lineages. Among these lineages, three Iranian lineages and one Uzbekistan lineage were suggested either as species or subspecies, respectively, while the other three were congruent with traditional morphological recognition, i.e., *E. v. velox* from most parts of Central Asia and western Xinjiang, China; *E. v. caucasia* from eastern Transcaucasia, northeastern Russian Caucasus and western Kazakhstan; *E. velox roborowskii* from the Turpan Depression in northwest China. Consequently, the lack of a comprehensive phylogenetic analysis of the lizard hindered the research on its biogeography (Liu et al., 2014), and, hence, our understanding of the evolutionary history of *E. velox*. To date, large gaps in geographic sampling in Central Asia still exist for this species, especially in the great arid landmass across Central Asia in Kazakhstan.

Our analyses were motivated by the goals to obtain a more detailed picture of the genetic structure of the population and to trace the population history of *E. velox* across its distribution range. We used a phylogeographic approach complemented with ecological niche modeling. Specifically, we aimed to (i) document the phylogeographic structure and the timing of genetic diversification within the rapid racerunner; (ii) reconstruct the center of origin and colonization routes; (iii) explore the relationship between historical demographic changes and past climate fluctuations; and (iv) test GM expansion versus GM contraction models for *E. velox*. Analyses of the mtDNA sequences tell only one part of a potentially more complex story (Ballard and Whitlock, 2004; Galtier et al., 2009), yet they provide valuable insights into the evolutionary history of a species, including consequences of habitat changes, impacts from climate fluctuations, and divergence and colonization. To incorporate the data published by Liu et al. (2014) and especially the data from the Iranian Plateau (Rastegar-Pouyani et al., 2012), we amplified the mitochondrial cytochrome *b* and 12S rRNA genes in this study.

2. Materials and methods

2.1. DNA extraction, amplification and sequence analysis

We analyzed 595 specimens of *Eremias velox* collected at 107 sites (Table S1; Fig. 1), from across its known distribution range. Of these, 155 specimens from 30 localities were taken from the studies of Rastegar-Pouyani et al. (2012) and Liu et al. (2014). A detailed list of information about all specimens and sequences is provided in Table S1.

Genomic DNA was extracted from ethanol-preserved liver or tail tissue samples using the universal high-salt procedures (Aljanabi and Martinez, 1997). Two mitochondrial genes coding cytochrome *b* (cyt *b*) and 12S rRNA were amplified. Detailed amplification and sequencing

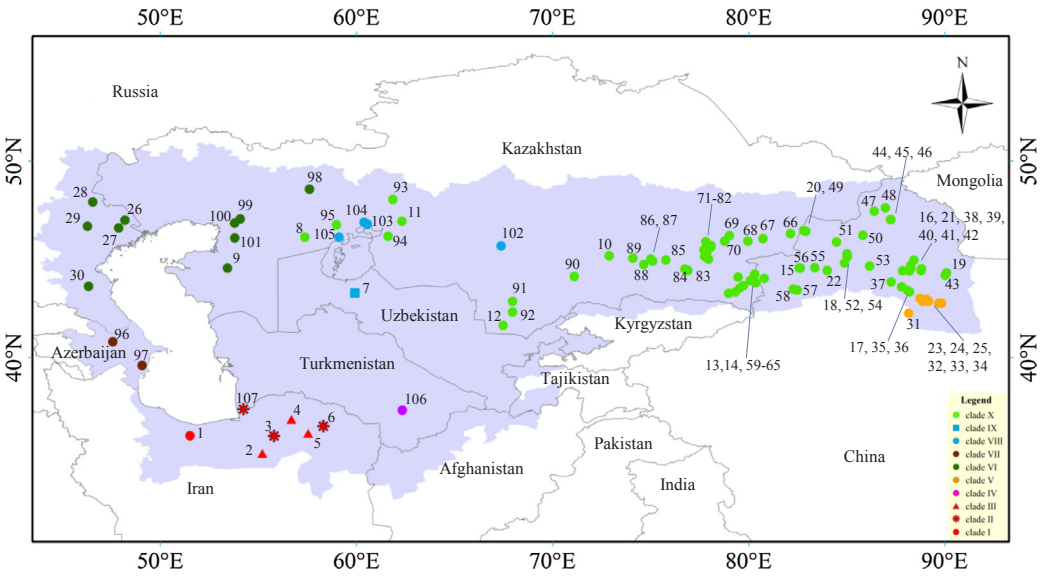

Fig. 1. Collection sites for the samples of *E. velox* used in this study. Sites are numbered as in Table S1 and clades are highlighted by different color. The background outlines the current distribution of *E. velox* according to Szczerbak (1974) and Sindaco and Jeremcěnko (2008). (For interpretation of the references to color in this figure legend, the reader is referred to the web version of this article.)

methods followed Liu et al. (2014). All PCR products were commercially purified, and sequenced for double strands. Sequences were deposited in GenBank with accession numbers MG478510–MG479389.

All novel cyt *b* gene sequences were translated into amino acid sequences using MEGA v7.0.26 (Kumar et al., 2016) to verify the data. Six outgroup sequences of *Eremias* lizards (*E. argus*, *E. persica* and *E. strauchi*) were retrieved from GenBank (Table S2). The produced sequences were aligned using Clustal X v2.0 (Larkin et al., 2007). No indel was found in cyt *b* matrices, while two indels were found in 12S rRNA matrices when outgroup sequences were included. The general characterizations of DNA variation and haplotypes were calculated in DnaSP v5.0 (Librado and Rozas, 2009).

2.2. Phylogenetic analysis

We used Bayesian inference (BI) and maximum likelihood (ML) to reconstruct phylogenetic relationships among the mitochondrial haplotypes. The dataset was first partitioned by genes, with the cyt *b* gene being separated into the following subsets: 1st, 2nd, and 3rd codon positions. We further used PartitionFinder v1.1.1 (Lanfear et al., 2012) to select the best partitioning strategy and the optimal nucleotide substitution model for the dataset using the Bayesian information criterion (BIC). A summary of DNA partitions and relevant models as determined by PartitionFinder is given in Table S3. Bayesian inference analysis was conducted using MrBayes v3.2.2 (Ronquist et al., 2012). Two independent runs were carried out with four Monte Carlo Markov chains (MCMCs) for 20 million generations with parameters and topologies sampled every 1000 generations. Convergence of the runs was assessed by the standard deviation of split frequencies (< 0.01). A 50% majority-rule consensus tree and posterior probability (PP) of clades were assessed by combining the sampled trees from the two independent runs after a 25% burn-in phase. All ML analyses were implemented in RAxML v8.2.4 (Stamatakis, 2014) under the GTR + G + I model with 100 replicates with a complete random starting tree. Bootstrap support (BS; Felsenstein, 1985) for the clades was assessed with a sufficient number of pseudoreplicates (450), which was automatically determined by using the default cutoff threshold. Additionally, the uncorrected *p*-distances of 12S rRNA and cyt *b* sequences were calculated with MEGA between and within each clade.

2.3. Molecular dating

We used a relaxed lognormal clock approach to estimate the divergence time of lineages as implemented in BEAST v1.7.5 (Drummond et al., 2012) based on the concatenated dataset. Due to a lack of reliable fossil evidence, we used secondary calibrations of robust divergence time calculations, choosing a two-step approach similar to that employed by Brandley et al. (2010). First, in order to introduce the calibration points, we retrieved the cyt *b* and 12S rRNA sequences from GenBank corresponding to 74 species in the Lacertidae family and one outgroup species (Table S2). We randomly selected one representative from each clade of *E. velox* reconstructed in the BI analyses (Fig. 2). We then combined the dataset to date the most recent common ancestor (MRCA) of *E. velox*. Models, priors and parameters are specified in Table S3. We set nine calibration points with a normal distribution of probability densities (Fig. S4). The first calibration point, C1, representing the MRCA of the subfamily Lacertinae based on the result of Pavlicev and Mayer (2009), was set at 13.75 ± 0.01 million years ago (Ma). C2, based on the result of Tseng et al. (2014) on the divergence times in the genus *Takydromus,* was set at 5.2 ± 0.9 Ma. For C3–C9, we used calibration points for other lacertids, *Gallotia* and *Podarcis*, as described in Tamar et al. (2016). In addition, we also employed the mean sequence evolution rates of the cyt *b* and 12S rRNA genes (as estimated in Carranza and Arnold, 2012) to cross-check the divergence time estimates of different taxa in the Lacertidae family.

In the second step, all sequences of *E. velox* were used to estimate the split time of interior lineages with the above age estimate for the MRCA of *E. velox* (6.23 ± 0.79 Ma). To ensure that the tree prior does not have a negative impact on molecular dating (Ritchie et al., 2017), we conducted analyses using two different tree priors, birth-death process and constant-size coalescent, for comparison with each other. Models, prior settings and parameters are listed in Table S3.

2.4. Ancestral area reconstruction

The possible ancestral range of *E. velox* was reconstructed by statistical dispersal-vicariance analysis (S-DIVA) and Bayesian binary MCMC (BBM) analysis in RASP v3.2 (Yu et al., 2015). Following the criteria used in Sanmartín (2003) and Shi et al. (2013), six areas were considered on the basis of paleogeographical history and environmental conditions in the distribution range of *E. velox*: (A) Iranian Plateau, (B) Turkmenistan, (C) Turpan Depression, (D) Transcaucasia, (E) Ciscaucasia and adjacent western Kazakhstan, and (F) Uzbekistan, Kazakhstan and northwestern China (Fig. 3). Thirty thousand trees previously produced in the BEAST run for the whole dataset of *E. velox* were used as the input file. Ten thousand random trees were selected after the first 10,000 trees were discarded as burn-in. We ran both analyses with default settings, except the number of maximum areas, which was set to

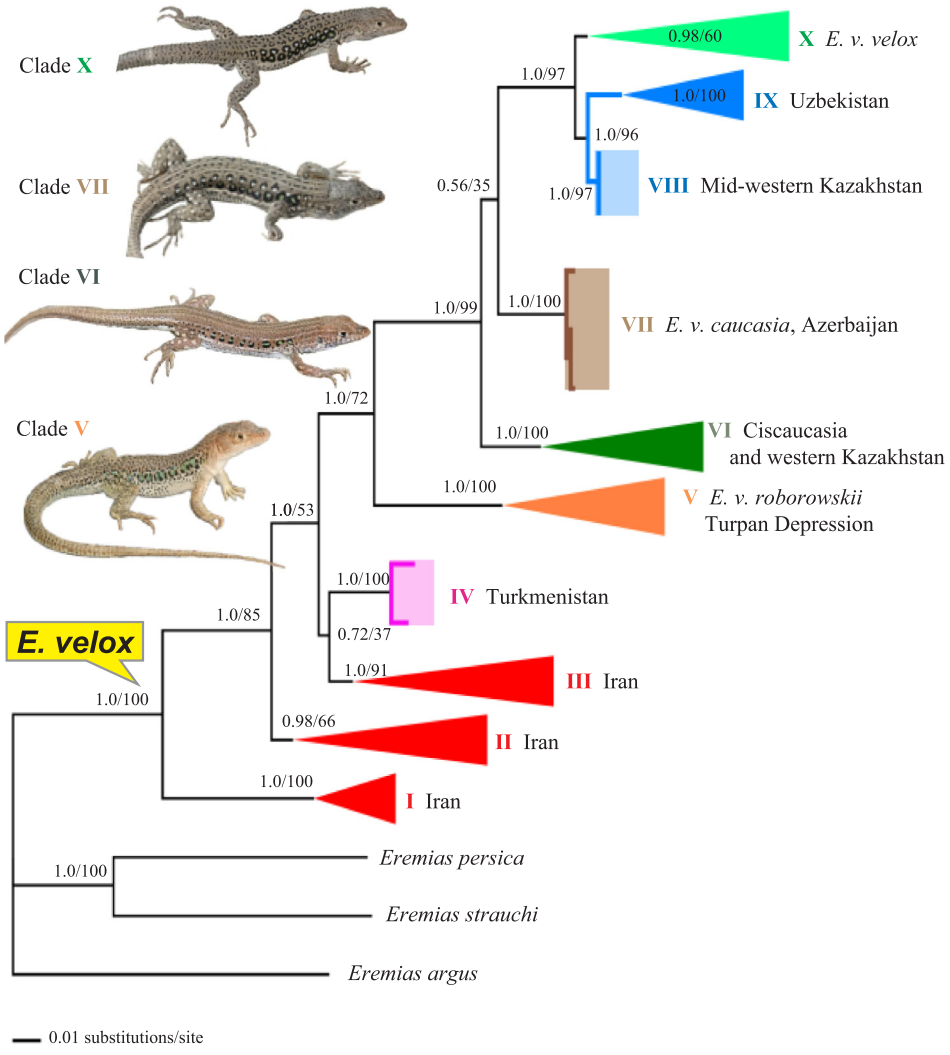

Fig. 2. Hypothesized relationships of *E. velox* included in this study, illustrated by the 50% majority-rule consensus tree resulting from partitioned Bayesian analyses. Bayesian posterior probabilities and maximum likelihood bootstrap values are shown. Colored alphabet labels correspond to clades referring to the Results and Discussion, which can be used to interpret Tables S1, S6 and S9. Representative photographs of male adults show the dorsal and lateral differentiation among four clades. *Eremias velox caucasia* (Clade VII) was redrawn based on http://www.lacerta.de/, photo by Torsten Panner. (For interpretation of the references to color in this figure legend, the reader is referred to the web version of this article.)

two in consideration of the limited dispersal ability of the lizard.

2.5. Population genetic analysis

We used DnaSP to calculate the number of haplotypes (*nh*), the haplotype diversity (*h*), the nucleotide diversities (π) and the average number of nucleotide differences (*k*) for each clade. We examined the spatial distribution of genetic variation within *E. velox* lineages using the analysis of molecular variance (AMOVA; Excoffier et al., 1992) in Arlequin v3.5 (Excoffier and Lischer, 2010). The statistical significance of the variance components in the AMOVA was tested with 10,000 permutations. In addition, we employed the inverse distance weighted (IDW) method to explore the geographic pattern of genetic diversity visually with ArcGIS v10.2 (ESRI, Redlands, CA, USA). Furthermore, to evaluate the genealogies of the haplotypes and their relatedness with their geographic origin, the median-joining network (MJN) reconstruction method (Bandelt et al., 1999) was applied for the two genetically defined subspecies of *E. velox* (i.e., Clade X for *E. v. velox*, Clade V for *E. v. roborowskii*) and the newly recognized Clade VI (see Results). Due to the small sample sizes for the other seven clades, we did not infer the haplotype network for them. The MJN method followed by the maximum parsimony (MP) option to clean up the network was implemented with NETWORK v4.6.1.3 (http://www.fluxus-engineering.com). To evaluate whether there is any geographic structure among haplotypes in the specific lineage, geographic subareas were defined according to the paleogeographic history and topography (see Fig. S1). Four subareas were defined for *E. v. velox*: (i) western Kazakhstan, (ii) southeastern Kazakhstan, (iii) Ily River Valley, and (iv) Junggar Depression; and two subareas were considered for Clade VI: Ciscaucasia and adjacent western Kazakhstan.

2.6. Bayesian species delimitation

We employed two distinct species delimitation methods (coalescent and non-coalescent statistical algorithms) to assess lineage separation in *E. velox*. First, we took a Bayesian implementation of the Poisson tree processes (bPTP) model (Zhang et al., 2013) as implemented on the bPTP server (http://species.h-its.org/ptp/) using a rooted consensus tree from the Bayesian phylogenetic analysis. We ran bPTP analyses twice with or without outgroup taxa included. The parameter settings were left as the default, except 300,000 generations were used for the MCMC. The convergence of the analyses was assessed with likelihood trace plots. Second, we employed a coalescent-based method with BPP v3.3 (Yang and Rannala, 2010). We used both A10 and A11 models (Yang and Rannala, 2014) to delimit the potential species. The consensus tree inferred from the above BEAST analysis was used as a guide tree. We assigned all of ten major clades as different putative species. Given that different priors favor models with fewer or more species, we checked different priors following the approach of Leaché and Fujita (2010). Reversible-jump Markov chain Monte Carlo (rjMCMC) algorithm 1 with the parameters combination (α, *m*) = (1, 0.5) and speciesmodelprior = 1 was used to repeat the BPP runs twice with

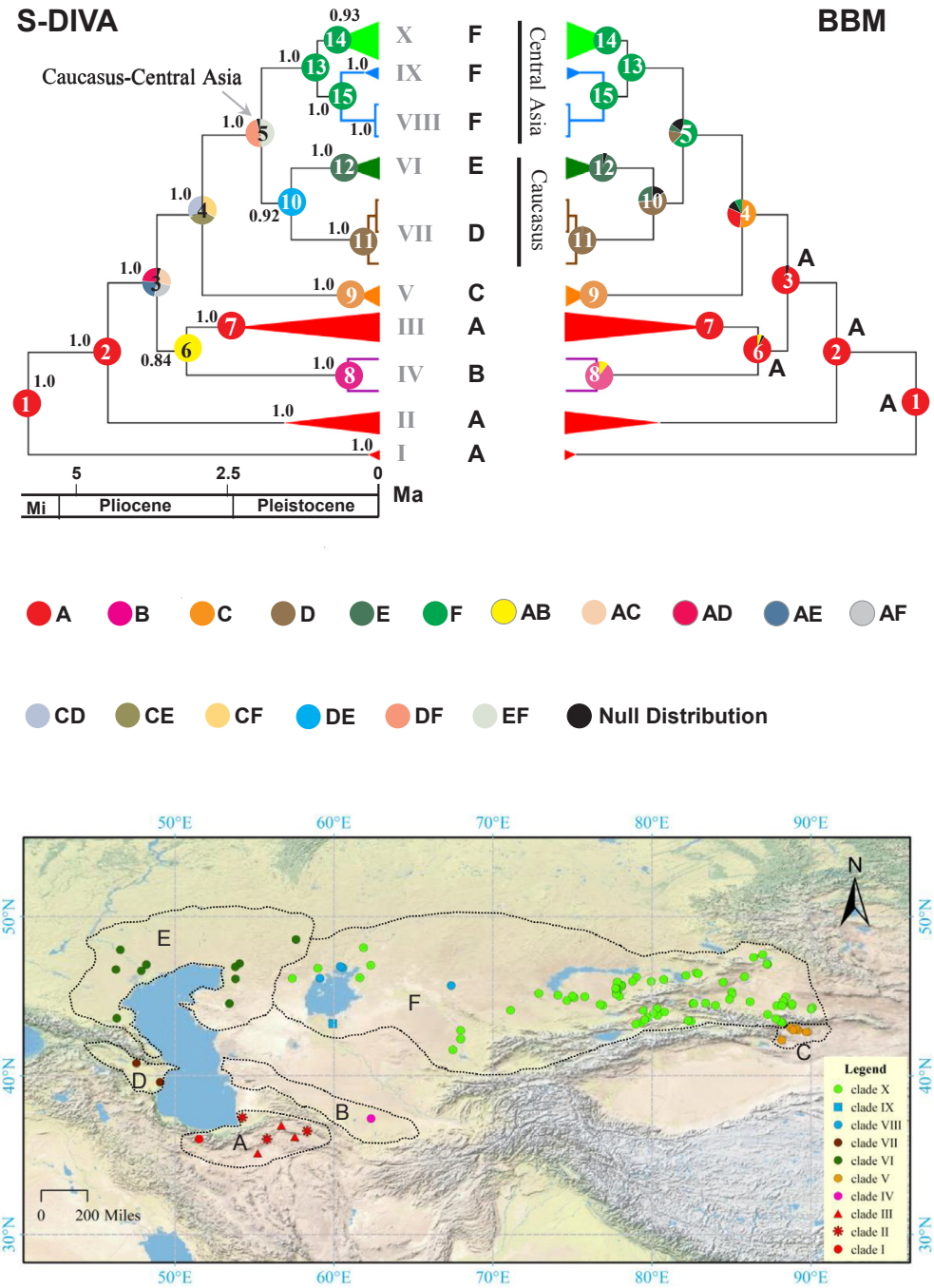

Fig. 3. Chronogram of *E. velox* based on the mitochondrial data and the estimated ancestral areas inferred from S-DIVA and BBM analyses. The main nodes on the tree are numbered as 1–15. Exact age estimates for all nodes are listed in Table S7. Mi, Miocene. Bayesian posterior probabilities are shown above the branches; results from S-DIVA and BBM analyses are shown on the left and right trees, respectively. Relevant proportional to the mean probability of the ancestral areas is filled as colored pie chart, with the statistical support for the ancestral areas and biogeographic events listed in Table S8. Symbols are plotted onto a map of arid Central Asia and adjacent regions, with color refers to mitochondrial lineage in Fig. 2. (For interpretation of the references to color in this figure legend, the reader is referred to the web version of this article.)

different starting seeds to assess the consistency between runs. The rjMCMC analysis was conducted for 100,000 generations in each run with a sampling interval of two and a burn-in of 4000.

2.7. Inference of demographic histories

Due to the small sample sizes of most clades, we conducted demographic analyses for the three clades (V, VI, and X) with three common methods, respectively. First, three types of neutrality tests were performed: (i) R_2 statistics (Ramos-Onsins and Rozas, 2002), with 1000 coalescent simulations to calculate the significance using DnaSP; (ii) Fu's *Fs* (Fu, 1997) and (iii) Tajima's *D* (Tajima, 1989), with significance tested using 10,000 bootstrap replicates with Arlequin. Second, mismatch distributions (MD) of pairwise nucleotide differences were calculated for the three clades using DnaSP, with 10,000 coalescent simulations. The goodness-of-fit between observed and expected distributions was tested by calculating Harpening's Raggedness index (*Rg*) and the sum of squares deviation (*SSD*). Third, extended Bayesian skyline plots (EBSP) were implemented in BEAST to estimate the changes in effective population size on an evolutionary time scale. We used the substitution rate of the 95% highest posterior density (HPD) interval inferred from the above BEAST analysis for the whole *E. velox* dataset; the lower bound was set to 2.6×10^{-8} per site per year, and the upper bound was set to 6.5×10^{-8} per site per year. Models, prior settings and parameters are listed in Table S3.

2.8. Present and past distribution modeling

We employed ecological niche modeling (ENM) to predict the distribution of major lineages during three periods, that is, at the present

time, the LGM (0.026–0.019 Ma) and the Last Interglacial (LIG; 0.14–012 Ma), and also to determine ecological divergence between each lineage. We used the maximum entropy algorithm to model the ecological niches of the species in MAXENT v3.3.3 (Phillips et al., 2006; Phillips and Dudík, 2008). Because there are very few occurrence localities in other lineages, which may prevent the reliable estimation of the model parameters (Phillips et al., 2006; Wisz et al., 2008), we focused on only two subspecies (i.e., Clade X for *E. v. velox*, Clade V for *E. v. roborowskii*) and the newly recognized Clade VI. We compiled 19 ecological variables (bioclimate variables) for each period from the WorldClim database (http://www.worldclim.org) (Hijmans et al., 2005), with a resolution of 2.5 arc-minutes for the LGM environmental layer, and 30 arc-seconds for the LIG and "present-day" environmental layers. For the LGM, we used the predictions of two general circulation models, i.e., community climate system model (CCSM) and the model for interdisciplinary research on climate (MIROC). Because strong colinearity between environmental variables could inflate model accuracy (Synes and Osborne, 2011), we excluded those variables with Pearson correlation coefficients $r > 0.85$ based on pairwise comparison of raster files in SDMtoolbox v1.1c (Brown, 2014). Eleven variables were retained for subsequent analysis (see Table S4). Georeferenced occurrence records were obtained from our field surveys. To ensure that input occurrence data are spatially independent and to reduce sampling bias, all sampling localities were also rarefied at a spatial distance of 10 km using SDMtoolbox in ArcGIS. Thus, the reserved occurrence points included 58 localities for *E. v. velox*, ten for Clade VI, and seven for *E. v. roborowskii* (Table S5).

Ecological niche models were constructed according to current environmental factors and then projected for the three different time periods. Maxent analyses were carried out with 70% of the species records for training and 30% for testing the model, 100 subsample replicates and 5000 iterations. The area under the receiving operator characteristics curve (AUC) was used to evaluate the performances of the models. Logistic thresholds of ten percent training presence that were generated in the Maxent output were used to define the minimum probability of suitable habitat. We then measured the niche differences between ecological niche models by calculating Schoener's *D* (Schoener, 1968) and Hellinger's *I* (Warren et al., 2008) in ENMTooLs v1.4.4 (Warren et al., 2010). We conducted an identity test to build niche models based on 100 pseudoreplicates generated from a random sampling of data points pooled for each pair of lineages. The observed measures of niche similarity between lineages were compared with the null distribution.

Principal components analysis (PCA) was conducted to compare niche differentiation between lineages to determine whether the genetic groups were ecologically differentiated. The PCA can convert a set of possibly correlated environmental variables into a set of values of independent variables. Principal components with eigenvalues > 1 that explained > 10% of the variation were retained. A permutational multivariate analysis of variance (MANOVA) implemented in SPSS v19.0 (SPSS, Chicago, USA) was conducted on all environmental variables simultaneously for each lineage pair and for the three lineages to evaluate whether environmental conditions differed significantly between their sites of occurrence because these may have been the drivers responsible for demographic and divergence patterns.

3. Results

3.1. Sequence characteristics and phylogenetic relationship

We generated a concatenated alignment comprising 1143 bp of cyt *b* and 373 bp of 12S rRNA (including indels) genes. A total of 598 concatenated sequences (including three outgroups) revealed 325 haplotypes. The dataset comprised 891 invariable sites (625 in cyt *b* and 266 in 12S rRNA), 615 polymorphic sites (518 in cyt *b* and 97 in 12S rRNA) and 495 parsimony-informative sites (421 in cyt *b* and 74 in 12S rRNA).

Bayesian inference and ML analyses produced highly congruent topology, with only minor conflicts on recent nodes (see Figs. S2, S3). Thus, only the BI tree with both PP and BS from ML is presented (Fig. 2; composition of haploclades is given in Table S1). Ten matrilineal lineages with strong PP and BS values were uncovered, except for the relatively low BS (60%) for Clade X and 66% for Clade II (Fig. 2). Most of the clades correspond to distinct geographic ranges; no haplotype was shared among the different subspecies. These lineages exhibited a significant difference in pairwise uncorrected *p*-distance (Table S6) in different genes (i.e., cyt *b* gene and 12S rRNA). Overall, the pairwise uncorrected *p*-distance in the 12S rRNA gene (Table S6.1) varied from 1.0% (VI and X) to 10.3% (I and IX) and was mostly lower than 5% between other clades. The 12S rRNA gene was more conservative among the lineages than the cyt *b* gene, which varied from 1.1% (VIII and IX) to 15.4% (I and X), with the latter mostly higher than 5% between other clades (Table S6.2). The relationship between the three Iranian geographic lineages (Clades I, II, and III) were similar to those in Rastegar-Pouyani et al. (2012). The relationship among III, IV and the remaining downstream clades (V–X) is unresolved via the data used. Clade V was restricted to the Turpan Depression and recognized as *E. v. roborowskii* by Liu et al. (2014). *Eremias velox roborowskii* formed the sister taxon to the Caucasus-Central Asia clade (including Clades VI, VII, VIII, IX and X), which is in accordance with that in Liu et al. (2014). Clade VI included populations from the Ciscaucasia and adjacent western Kazakhstan, corresponding to the previously recognized *E. v. caucasia* in Liu et al. (2014). However, the relationship among VI, VII and VIII-IX-X is unresolved due to the low PP (0.56) and BS (35%). Clade VIII, comprising three populations from the northern bank of the Aral Sea and one from central Kazakhstan, formed the sister taxon to Clade IX, which was previously recognized as an Uzbekistan lineage in Rastegar-Pouyani et al. (2012). Clade X, encompassing the broadest range, including western and southeastern Kazakhstan as well as western China, is traditionally recognized as the nominate form *E. v. velox* (Szczerbak, 1974, 1975, 2003).

3.2. Timeframe for the diversification of E. velox

Our two different Bayesian dating analyses that employed calibration points and substitution rates yielded congruent results (see Figs. S4, S5). However, Bayes factor (BF) (Kass and raftery, 1995) strongly favored the calibration point approach over the substitution rate approach (2lnBF > 400). Hence, we preferred the estimates of divergence time based on calibration point. The results indicated that the MRCA of *E. velox* and the closely related outgroup diverged approximately 9.72 million years ago (Ma) [95% highest posterior density interval (HPD), 7.71–11.85 Ma] (Fig. S4). As shown in Fig. S4, the MRCA of *E. velox* was dated in the Late Miocene (6.23 Ma; 95% HPD, 4.66–7.91 Ma). The molecular dating for the major splits of *E. velox* yielded similar results with the two different tree priors (see Table S7). However, the birth-death process outperformed the constant-size coalescent tree prior (2lnBF > 460). Hence, we preferred the results with the birth-death process to the constant-size coalescent (Fig. 3). Clades I and II diverged during the Late Miocene-Early Pliocene. The Iranian Clade II diverged at approximately 4.58 Ma. Clade V (*E. v. roborowskii*) diverged from the Caucasus-Central Asia clade (comprising Clades VI–X) approximately 2.99 Ma (node 4). Subsequent rapid divergence events occurred in the Quaternary.

3.3. Ancestral geographic distribution

The ancestral area reconstructions of *E. velox* by S-DIVA and BBM are shown in Fig. 3, with the different optimal historical area reconstructions indicated at the nodes. The BBM reconstructions for terminal (3, 4, 5) nodes were more restricted than those of S-DIVA. The most parsimonious scenario was postulated in the S-DIVA analysis with six dispersals (colonization events), five vicariances (allopatric

divergence events) and one extinction, while this occurred in the BBM analysis with ten dispersals, five vicariances and 0 extinctions (Table S8). As shown in Fig. 3, both analyses indicated that *E. velox* may have originated from the Iranian Plateau (area A) with strong statistical support. Although the ancestral area of the clade comprising Clades III–X (node 3) was not clear in the S-DIVA analysis, the BBM analysis apparently pointed to the ancestral area in Iran (A), which suggested that *E. velox* dispersed into Central Asia from the Iranian Plateau. Iran (A) was inferred as the ancestral area for the lineage (node 6) leading to Clade III and Clade IV in the BBM analysis, while S-DIVA analysis indicated Iran (A) and Turkmenistan (B) as the ancestral area of node 6. The ancestral area of Caucasus-Central Asia clade (node 5) was deciphered as DF (P = 46.48%) or EF (P = 49.44%) in S-DIVA analysis, while the BBM analysis indicated that the most possible ancestral area was F (P = 62.53%). The BBM analysis assumed that the ancestral area of the Caucasus clade (node 10; including Clades VI and VII) was distributed in area D (P = 59.28%) or E (P = 26.09%), while the S-DIVA analysis showed DE as the ancestral range of the Caucasus clade. Both the S-DIVA and BBM analyses inferred F as the ancestral areas for nodes 13–15.

3.4. Genetic diversity and genetic structure

The genetic diversity indices are given in Table S9. The nucleotide diversity of the mtDNA was 4.21% and ranged from 0.07% (Clade VIII) to 3.72% (Clade III) among the clades. The geographic patterns of the genetic diversity interpolated using the IDW method are shown in Fig. S6, with the highest genetic diversity distributed in Iran. AMOVA showed a maximum percentage of variance (93.74%) when the populations were grouped into ten clades (Table S10). The variances between sampled localities (populations) within clades and within populations were 3.03% and 3.23%, respectively. When the Caucasus-Central Asia clade was considered one group, significant genetic structure still existed among groups (Φct = 0.87, $P < 0.001$), with 86.99% variance (Table S10).

For *E. v. velox* (Clade X), the MJN produced a complex pattern (Fig. S7a), with the network comprising multiple configurations, including one star-like network, with the central sequences being the most frequent haplotype (Hap45). Although 205 haplotypes were detected, the network shows relatively shallow genetic divergence and little evidence of an overt geographic structure. For Clade VI, a similar network structure to *E. v. velox* was detected, exhibiting no apparent geographic structure rather than a star-like topology (Fig. S7b). Haplotypes from western Kazakhstan were at least eight mutational steps away from the haplotypes in the Ciscaucasia. Likewise, no geographic structure among the populations from the Turpan Depression was detected in the MJN for *E. v. roborowskii* (Fig. S7c).

3.5. Species delimitation

We repeated the BPP analysis 12 times under a variety of different algorithms, prior distributions and starting seeds. The convergence between two independent runs using different starting seeds was assessed, and then we combined the two runs to assess the posterior probabilities under different species delimitation models. For both the A10 and A11 models, analyses under a prior combination of $\theta \sim$ G (2, 2000) and $\tau_0 \sim$ G (2, 2000) recognized ten genetic structures with strong support (PP > 0.95), while under a prior combination of $\theta \sim$ G (1, 10) and $\tau_0 \sim$ G (2, 2000), Clades VIII and IX may form one species with low PP support in both (0.309 in A10, 0.288 in A11) (Table S11). For the A10 model, analysis under a prior combination of $\theta \sim$ G (1, 10) and $\tau_0 \sim$ G (1, 10) supported full species delimitation with strong support (PP = 0.986), while for the A11 model, the analysis supported nine species scenarios with low support (PP = 0.355). However, the bPTP analysis identified only five out of ten clades as distinctive species with relatively high support, i.e., Clade I (PP = 0.85), Clade V (*E. v. roborowskii*; PP = 0.91), Clade VII (PP = 0.84), Clade VIII (PP = 0.97), and Clade IX (PP = 0.77) (Fig. S3).

3.6. Historical demographic change

Clades X, VI, and V showed similar results for Tajima's *D*, Fu's *Fs* and R_2. For Clade X (*E. v. velox*) and Clade V (*E. v. roborowskii*), the values of Fu's *Fs* and Tajima's *D* were negative and statistically significant, as well as the significantly small R_2 value (Table S9), indicating demographic expansion. Clade VI presented a non-significantly negative Fu's *Fs* value but significantly negative Tajima's *D* and small R_2 values, indicating demographic expansion. The MD analysis of Clade X suggested a clear recent history of population expansion, as indicated by the typical smooth, unimodal distribution (Fig. S8), consisting of low and significant *SSD* but nonsignificant *Rg* values (Table S9). Clades V and VI were characterized by multimodal and ragged and erratic MD (Fig. S8), while both exhibited nonsignificant *Rg* values, indicating a scenario of demographic expansion (Table S9). The demographic scenario for *E. velox* determined through EBSP analyses suggested different patterns for the three clades. The EBSP estimates of Clade X visualized changes in the effective population size over time, revealing a two-stage increase in the effective population size of *E. v. velox* during the Pleistocene (Fig. 4). The effective population size of *E. v. velox* has detected an expansion event commencing approximately 0.25 Ma, reaching the peak at approximately 80 ka, then following a bottleneck event ending approximately 24 ka, finally following a rapid expansion (Fig. 4). The EBSP estimates of Clade V suggested that the population has expanded approximately nine-fold, beginning at approximately 0.025 Ma, with no evidence of contraction afterwards. In contrast, Clade VI showed a stable condition in terms of the effective population size during the LIG and the LGM, along with a recently weak demographic expansion since the beginning of the Holocene (Fig. 4).

3.7. Ecological niche modeling

The predicted distributions of the three clades (X, VI, V) during the LIG, LGM, and the present day are illustrated in Fig. 5. For each distribution model, the AUC value approached one (≥0.95), indicating a better than random prediction. In addition, the projected present-day distribution is consistent with collection records. For the LGM period, the two general models, CCSM and MIROC, predicted largely incongruent results. We took the results of the CCSM model as reliable predictions, as the estimations (Fig. 5) were in accordance with our expectations and the estimations for suitable habitats from the MIROC model were outside of the possible distribution ranges of *E. velox* (Fig. S9). The predicted distributions showed that the suitable range for *E. v. velox* expanded across the Caucasus, western and southeastern Kazakhstan, western China and even the Iranian Plateau during the LIG, while the habitats almost vanished in all areas except for a small part in southern Ciscaucasia and a minor area in the Ily River Valley in Kazakhstan, possibly in response to climatic cooling during the LGM. However, the current areas of predicted *E. v. velox* presence expanded to western Kazakhstan, southeastern Kazakhstan and western China. For Clade VI, the predicted distribution range during the LIG covered most part of Transcaucasia and the eastern edge of the Greater Caucasus Mountains near the coast of the Caspian Sea, and other territories that are unlikely to be occupied by Clade VI. During the LGM, the suitable habitats largely contracted to the southwestern shores of the Caspian Sea, while the current areas of the predicted presence range covered the Caucasus and adjacent western Kazakhstan. For *E. v. roborowskii*, the predicted distribution range was constrained to the Turpan Depression during the LGM and present, except implausible areas predicted in the LGM, such as western Kazakhstan and the northern Tarim Basin. During the LIG, the predicted habitats seemed to encompass areas north of foothills of the Tianshan Mountains in the Turpan Depression to most part of the Junggar Depression.

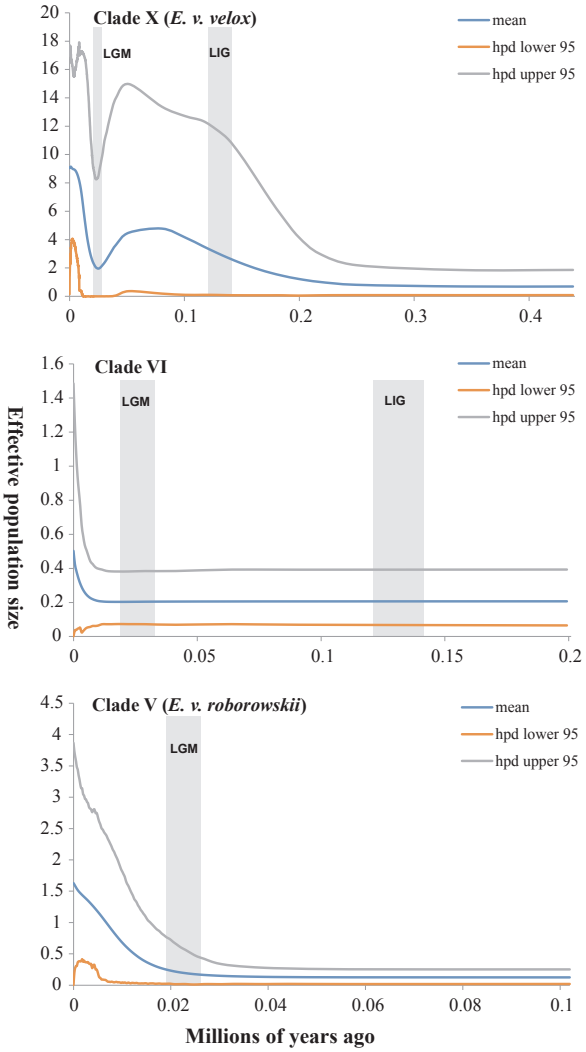

Fig. 4. Extended Bayesian Skyline Plots show the demographic trends in the three clades (X, VI, V). The y-axes represent the estimated effective population size on a log scale ($N_e\tau/10^6$, the product of the female effective population size and generation length in years); x-axes represent time in millions of years ago (Ma). Vertical dark-grey bars represent the duration of the last glacial maximum (LGM), or the last interglacial (LIG). (For interpretation of the references to color in this figure legend, the reader is referred to the web version of this article.)

Ecological niche identity tests confirmed the existence of niche differentiation between the three lineages (i.e., Clades X, VI, V) (Fig. 6a). ENMTOOLS showed that empirically observed values for *I* and *D* were significantly lower than those expected from the pseudoreplicated dataset in all paired analyses (Clade X vs. VI, VI vs. V, V vs. X, $P < 0.01$). Principal component analysis showed that 69.30% of the total variance was explained by the first two principal components (PC1: 44.94%, PC2: 22.36%, respectively) (Table S4). The first principal component represented precipitation and temperature (the lower the value, the colder and drier), while the second principal component represented climatic variability (the lower the value, the less variable). Habitats for Clade V (*E. v. roborowskii*) appeared to be cooler, drier and more variable than those for Clade VI and Clade X (*E. v. velox*) (Fig. 6b). The MANOVA conducted on 11 variables distinguished significant differences between three lineages with regard to environments occupied (Wilk's $\lambda = 0.409$, $F = 16.332$, $P < 0.001$). This result provided ecological and physiographic explanations for the distinct demographic histories of each lineage.

4. Discussion

4.1. Origination from the Iranian Plateau and the initial diversification

This study provides strong support for the hypothesis that *E. velox* originated from the Iranian Plateau and then dispersed into Central Asia, which is consistent with the results of Rastegar-Pouyani et al. (2012). The extremely high genetic diversity in Iran (see Table S9; Fig. S6) also suggests this area as a potential center of origin for *E. velox*. However, congruent with the divergence time estimate for *E. velox* in Guo et al. (2011) at 5.3 ± 1.4 Ma, our molecular dating with respect to the MRCA age of *E. velox* at ~6.23 Ma (4.66–7.91 Ma) postdates the previous rough estimate (10.7 ± 1.4 Ma) by Rastegar-Pouyani et al. (2012). This difference could be explained using different approaches and calibration points. We believe that using Bayesian molecular dating by considering variations in rates of change across lineages (relaxed molecular clock), not just rate constancy ("strict clock"), as in Rastegar-Pouyani et al. (2012), is one of the best currently available alternatives. The divergence time estimates indicate that genetic split among most lineages of *E. velox* occurred during the Late Miocene and Pleistocene. Although caution is needed when interpreting these results because of the poor paleogeographical data and fossil records, the estimated timescales for the inferred historical events are congruent with the known geological and climate scenarios for the geographic areas (see discussion below).

As noted by Rastegar-Pouyani et al. (2012) and Liu et al. (2014), the separate coalescence of the Iranian clades most likely resulted in allopatry during past periods of geographic isolation. Furthermore, the separation of the different lineages in Iran seems to fit the topography of the country. The geographic division between Clade I and Clade II/Clade III coincides with the Alborz Mountains. Thus, the divergence times and the phylogenetic patterns (Fig. 3) support the assumption that the evolutionary history of *E. velox* on the Iranian Plateau was correlated with the formation of isolated habitats due to aridification during the rapid uplift of the west-central Alborz Mountains by *ca.* 6 Ma (Axen et al., 2001).

Although our S-DIVA analysis did not decipher the most possible ancestral area for the clade, including Clades III–X (node 3 in Fig. 3), the BBM postulated that the ancestral area was in Iran with 95.92% marginal probability, which indicated that the populations from Iran dispersed into the territory of Central Asia (P = 0.46; Table S8). This scenario promoted us to assume that some Clade III-like ancestral populations invaded Central Asia via the land bridge between the Caspian Sea and the Badkyz and Pamir Plateaus, where they had evidently become arid as a result of the regressions of the Caspian Sea during the Pliocene Productive Series (Axen et al., 2001; Forte and Cowgill, 2013; Popov et al., 2010). Based on a correlation to an oxygen-isotope record, the ages of the Productive Series was estimated as 5.9 Ma and 3.1 Ma for the lower and upper boundaries, respectively (Abreu and Nummedal, 2007). In the Mid-Pliocene, the lizards seemed to have dispersed into Central Asia rapidly owing to unoccupied niches and lack of ecological competitors. This fits well with a scenario of further intensified desertification in ACA during the Late Pliocene (Lu et al., 2010). The expanding arid habitat in ACA provided an opportunity for dispersal of the ancestral populations of *E. velox*, and may facilitate the arid-adapted lizards to radiate into this vast territory.

Although the relationship among Iranian Clade III, Turkmenistan clade IV and the remaining downstream (V–X) clades is unresolved, these clades diverged at approximately 3.75 Ma (node 3 in Fig. 3), which coincided well with the most intense uplifting of the Kopet-Dagh Mountains at approximately 3–4 Ma (Shabanian et al., 2009). Therefore, the barrier of gene flow between the populations from Iran and Central Asia may be correlated with the uplifting of the Kopet-Dagh Mountains in the Late Pliocene. The dispersal of Clade IV to the north was obviously limited by the Pra-Amudarya River, which flowed from the uplifting Hindikush Mountains to the southeastern coast of the

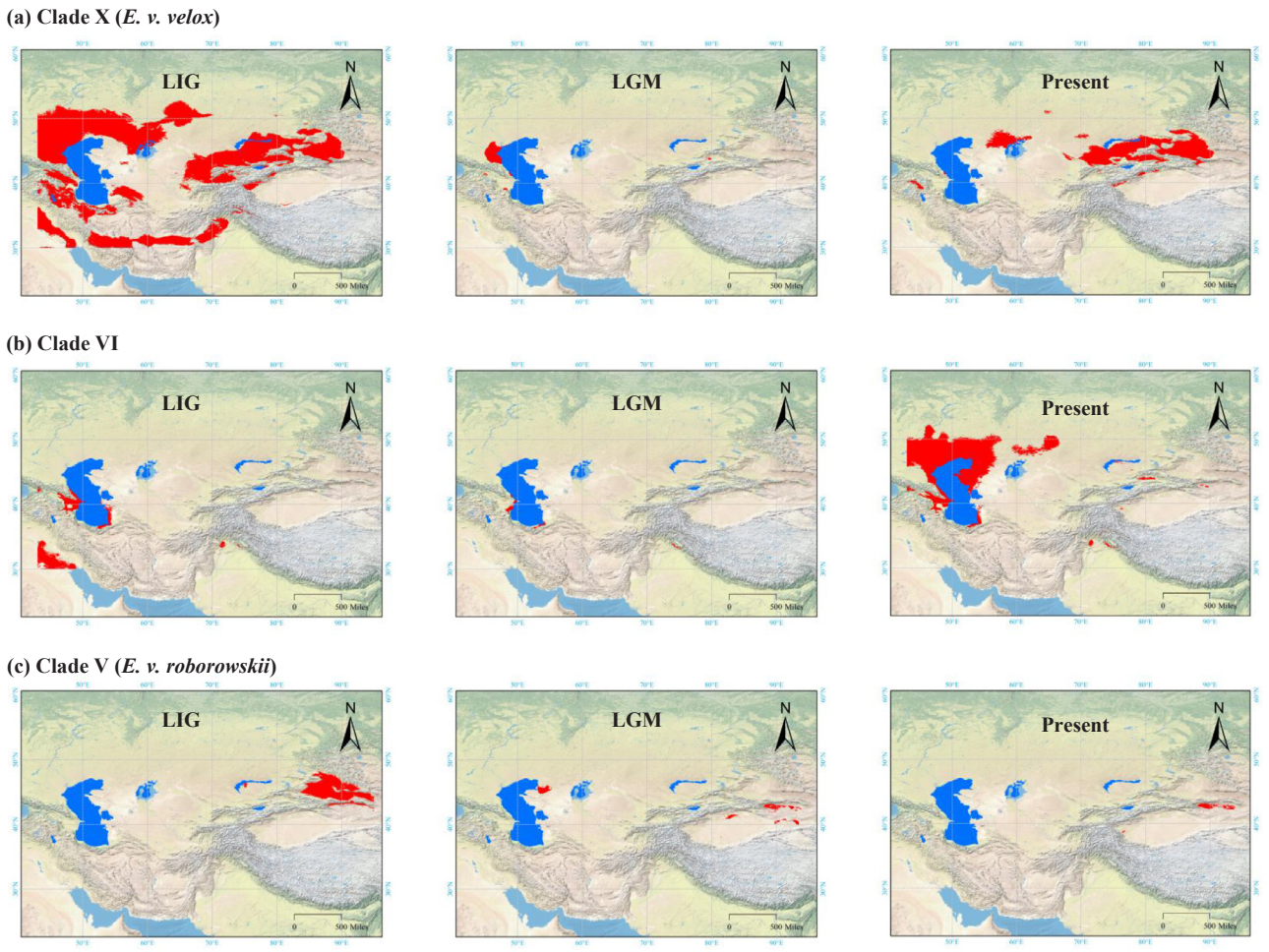

Fig. 5. Projected distributions of the three clades (X, VI, V) during the LIG, the LGM, and the present-day across arid Central Asia. Red color on the maps indicates predicted distribution areas, as the average values of ten percentile training presence logistic thresholds are 0.3942 for Clade VI, 0.1911 for Clade V (*E. v. roborowskii*) and 0.3097 for Clade X (*E. v. velox*), respectively. (For interpretation of the references to color in this figure legend, the reader is referred to the web version of this article.)

Caspian Sea in the Middle-Late Pliocene (Atamuradov, 1994).

The origin of *E. v. roborowskii* appears to reflect further eastern colonization of rapid racerunners via the Turkestan ridges and/or the dry Eastern Paratethys Sea towards the Tianshan Mountains. The divergence time between *E. v. roborowskii* (Clade V) and the Caucasus-Central Asia clade (node 4 in Fig. 3) was dated at approximately 2.99 Ma, which coincides well with the youngest rapid uplift of the Bogda Mountain from the eastern Tianshan Range at ~3 Ma (Wang et al., 2015). This allopatric divergence is likely associated with vicariance (P = 0.32; node 4 in Table S8) caused by the intense uplift of the Tianshan Mountains in the Late Pliocene (Trifonov et al., 2012). Some populations were trapped in the Turpan Depression and eventually gave rise to the current *E. v. roborowskii*, which had shifted its niche towards more arid habitats at lower altitudes (Fig. 6b). Those lineages in Central Asia/Caucasus became the Caucasus-Central Asia clade (e.g., *E. v. velox*, *E. v. caucasia*), thus being geographically separated from *E. v. roborowskii*.

4.2. Pleistocene glaciations, repeated transgressions of the Caspian Sea, and further diversification of the Caucasus-Central Asia clade

One of the most important findings in this study is that the diversification of the Caucasus-Central Asia clade appears to have been further molded by Pleistocene glaciations along with the repeated transgressions of the Caspian Sea. The coalescent time of this clade was dated to approximately 2.05 Ma (node 5 in Fig. 3), fitting well with the onset of the Northern Hemisphere glaciations approximately 2.7 Ma (Raymo, 1994).

Glacial cycles are responsible for the major transgressions and regressions of the Black and Caspian Seas in the ancient Paratethyan region (Ryan et al., 2003; Sorokin, 2011; Forte and Cowgill, 2013). The initial separation of the Black and Caspian basins dates to approximately 3 Ma (Tudryn et al., 2013). From that time, recurrent transgressions led to reconnections of the two basins. The period 3.75–2.45 Ma (nodes 3 and 7 in Fig. 3) roughly falls within the time frame of the periodic flooding of the Middle Caspian (Forte and Cowgill, 2013). This temporary drop in sea level appears to have allowed the lineage leading to node 5 (perhaps having the range DEF) to reach the Caucasus region (areas DE) from Central Asia (area F). Subsequently, at approximately 2.05 Ma, a possible allopatric subdivision of the ancestral range at node 5 gave rise to the clades leading to node 10 and node 13 (see Fig. 3). Glaciations could facilitate the diversification of the Caucasus-Central Asia clade through the Akchagylian transgression (3.4–1.6 Ma) of the Caspian Sea (Abreu and Nummedal, 2007; Jones and Simmons, 1996; Steiniger and Rögl, 1984), creating the geographic barrier between the populations from the Caucasus Mountains and Central Asia.

It is well acknowledged that the Caucasus region harbored glacial refugia during Pleistocene for diverse fauna and flora taxa (e.g., Arnerup et al., 2004; Dubey et al., 2006; Grassi et al., 2008; Neiber and Hausdorf, 2015; Tarkhnishvili et al., 2001). Our ENM analyses indicate that eastern Caucasus acted as potential refugia during the LGM for

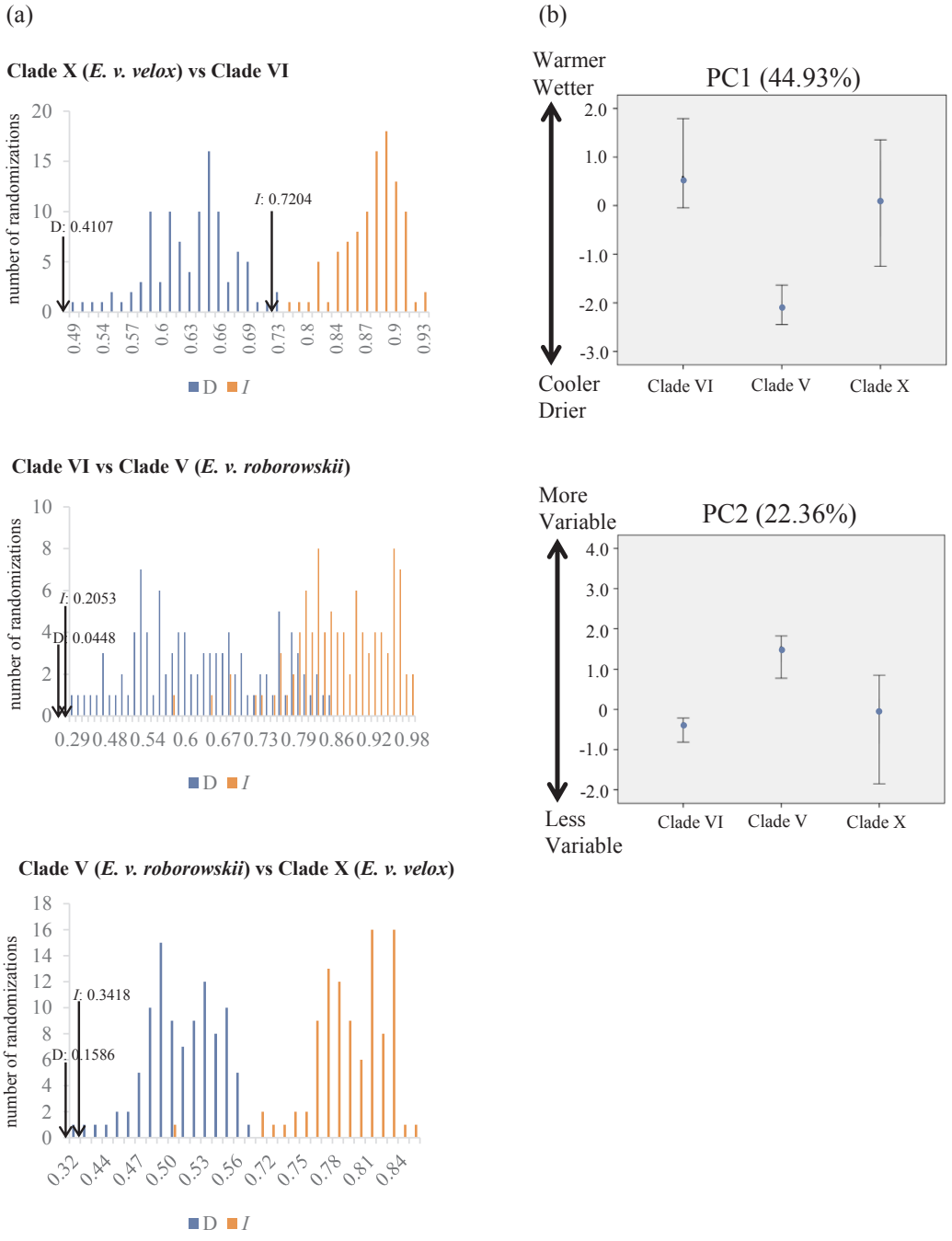

Fig. 6. (a) The results of a niche identity test between the three clades (X, VI, V) of *E. velox*, and (b) the results from comparison of environmental (means ± 95% CIs) conditions at sampling sites for the three clades. The x-axis indicates the value of *D* and *I*, while the y-axis shows the number of randomizations. The arrow indicates the value in actual Maxent runs. Habitats where Clade V occurs are significantly cooler, drier and more variable than those occupied by Clade VI and Clade X. (For interpretation of the references to color in this figure legend, the reader is referred to the web version of this article.)

Clade X (*E. v. velox*) and Clade VI, while another predicted refugium for *E. v. velox* was located in the Ily River Valley (Fig. 5). On the one hand, if we consider the southeastern Ciscaucasia as a potential refugium for *E. v. velox*, this requires the following additional assumptions: (i) the existence of undiscovered populations of *E. v. velox* in this area, or (ii) all populations of *E. v. velox* in this area became extinct except for those that colonized eastward after the LGM. On the other hand, if we consider niche conservatism (Peterson et al., 1999; Wiens and Graham, 2005), the above first assumption is rejected because southeastern Ciscaucasia hosts suitable habitat for Clade VI, and the niches of *E. v. velox* and Clade VI differentiated significantly from each other (Fig. 6). After the LGM, boreal glacial lakes drained south to the Caspian Sea through the Volga River; this caused an extensive transgression and the northern margin of the Caspian Sea reached the present middle Volga River (Tudryn et al., 2013). Either the Caspian Sea overflowed to the Black Sea through the Kuma-Manych Strait (Dolukhanov et al., 2010) or ice-marginal lakes provided connections between the Caspian Sea and the Arctic Ocean via the ancient Turgai Strait (Väinölä et al., 2001). Hence, the possibility of populations colonizing eastward after the LGM is excluded. In addition, we observed ancestral haplotypes for Clade X not in western Kazakhstan but the Ily River Valley and Junggar Depression (Fig. S7a). Thus, we consider the Ily River Valley to be a plausible refugium for Clade X.

In the Caucasus clade, the divergence of Clades VI-VII was estimated

to be approximately 1.48 Ma (node 10; Fig. 3), fitting well with the intense uplift of the Greater Caucasus Mountains during the Pleistocene (Mosar et al., 2010). The Greater Caucasus chain has been identified as a major barrier hampering the dispersal of Ciscaucasia by animals from Transcaucasian refugia (Dubey et al., 2006; Manceau et al., 1999; Seddon et al., 2002; Tarkhnishvili et al., 2000). Accordingly, it seems implausible that there were potentially suitable habitats in the Transcaucasia for Clade X (*E. v. velox*) and Clade VI during the LIG (see Fig. 5). If so, Clade VI may be restricted to only the narrow belt of foothills of the eastern Greater Caucasus Mountains along the coast of the Caspian Sea, while *E. v. velox* may have widely spread across Ciscaucasia, western and southeastern Kazakhstan, and western China during the LIG.

The ensuing evolution of the Central Asia clade may have been caused by the repeated retraction and expansion of the population ranges in response to Quaternary glaciations, along with rapid sorting of ancestral polymorphisms and local adaptation. Populations from the VIII, IX and X clades probably came into secondary contact in midwestern areas of Kazakhstan. One mechanism that may have contributed to the establishment and maintenance of the boundaries between the clades through the midwestern Kazakhstan is transgressions of the Caspian Sea. The midwestern areas of Kazakhstan were strongly influenced by the sea level changes in the Caspian Sea during the Pleistocene and Holocene, with some transgressions surpassing present-day sea levels (Forte and Cowgill, 2013; Mamedov, 1997; Rychagov, 1997). The vicariance event between Clade X and Clades VIII and IX at approximately 1.03 Ma (HPD 0.48–1.61 Ma) (node 13; Fig. 3) may have been triggered by the Apsheronian transgression of the Caspian Sea from *ca.*1.8 Ma to 0.7 Ma (Abreu and Nummedal, 2007; Green et al., 2009; Jones and Simmons, 1996; Steiniger and Rögl, 1984; Zubakov, 2001). The VIII-IX divergence (~0.63 Ma) within area F (node 15; Fig. 3) may be associated with several transgressive episodes in the Caspian Sea in the Holocene, which were dated to approximately 8 ka, 7 ka, 6 ka and 3 ka (Rychagov, 1997). The populations of *E. v. velox* in western Kazakhstan may be recently derived populations, as *E. v. velox* spread westward from its refugia in the Ily River Valley. This assumption is confirmed by the haplotype network of *E. v. velox* (see Fig. S7a), which indicated that haplotypes from western Kazakhstan occupied the tip positions.

4.3. Lineage-specific response to Quaternary climate oscillations

Responses to Pleistocene glacial cycles are expected to vary among species/lineages and geographical regions, in part because of differential cold/arid tolerance (Hewitt, 1996, 2004). Our analyses revealed a complex phylogeographic history for *E. velox*, with different demographic processes affecting each of the major lineages (Clades X, VI, V). This difference may have been due to the different populations/lineages of *E. velox* having different biological attributes and/or because the environmental conditions during glaciations were different in different distribution areas of the species. The phylogeography inferred from the mtDNA has a resolution restricted to the timespan of the Pleistocene, while the integrated frequency analyses of haplotypes, EBSP and ENM provide novel insights into the demographic history of the species.

During the Plio-Pleistocene, the climatic conditions in the mountains and plains of Central Asia varied repeatedly (Aubekerov and Gorbunov, 1999). The expansion of permafrost across the plains of Kazakhstan during the LGM (Vandenberghe et al., 2014) would have promoted distribution contractions or shifts and population isolation. On the other hand, island patterns of Pleistocene lowland permafrost in Central Asia, as low as 900 m a.s.l. (Aubekerov and Gorbunov, 1999), potentially left space for scattered Pleistocene refugia for arid-adapted lizards. During glaciations, *E. v. velox* took potential refugia in the Ily River Valley where there were semiarid deserts and steppes, while Clade VI retreated further south into the foothills of the eastern Greater Caucasus Mountains and Transcaucasia near the coast of the Caspian Sea (see Fig. 5). Geographically, however, the main thrust of the Greater Caucasus Mountains intruded eastward into the coast of the Caspian Sea near Transcaucasia (Mosar et al., 2010), which may have acted as geographic barriers for populations of Clade VI to disperse into Transcaucasia. Therefore, the areas occupied by Clade VI occupied during the LGM may have been restricted to only the foothills of the eastern Greater Caucasus Mountains near the coast of the Caspian Sea.

Haplotype diversity (h) and nucleotide diversity (π) can reveal the general demographic history of populations (Avise, 2000). Clade VI showed high h and low π, which suggests population growth from an ancestral population (see Table S9). Moreover, a star-like network suggests that the Clade VI might have experienced recent expansion (see Fig. S7). Furthermore, the EBSP shows that the Clade VI was stable during the LIG and the LGM, along with expansion starting at 10 ka after the LGM (see Fig. 4). This finding is congruent with the ENM analyses, which indicated present substantial range expansions (see Fig. 5). Likewise, for *E. v. velox*, rapid range expansions are supported by a similar star-shape network with a level of high h and low π (see Table S9). This result is consistent with the significantly negative Tajima's *D* and Fu's *Fs* statistics and the mismatched distributions for *E. v. velox*. The EBSP analysis even depicts a clear temporal scenario of the demographic history of *E. v. velox*, with population expansion during the LIG, then a population bottleneck following during the LGM, and finally population expansion again after the LGM. This scenario is also highlighted by our ENM analyses, which show a wide distribution of *E. v. velox* during the LIG, a restricted distribution in the Ily River Valley during the LGM, and current widespread distribution in western Kazakhstan, southeastern Kazakhstan and western China. Thus, niche modeling and phylogeographic analyses indicate that *E. v. velox* persisted through the LGM in very limited suitable habitats in the Ily River Valley (potential refugia) and achieved its current wide distribution via westward, northward and eastward dispersal after the retreat of the permafrost. Taken together, both Clade VI and *E. v. velox* apparently underwent substantial range and population size expansions after the LGM, which is consistent with the predictions of the GM contraction model (Hewitt, 2004).

The arid-adapted species in the desert in northwestern China might have been primarily influenced by climate cooling and changes in the precipitation regime instead of glaciers covering the areas adjacent to their distribution areas (Cheng et al., 2017; Wang et al., 2013). In the Eastern Tianshan Mountains, because of the extra continental climate, glaciers/permafrost did not advance below 2400 m a.s.l. during the LGM (Shi et al., 2006). *Eremias velox roborowskii* is restricted to the Turpan Depression, which is the second lowest place in the world at 155 m below sea level. Hence, the suitable habitats for *E. v. roborowskii* were not covered by ice during the LGM. Ecological niche modeling suggests that this low-elevation lineage is more cold/arid-tolerant than the other two lineages (Clade VI, Clade X) (Fig. 6b). If true, then *E. v. roborowskii* is less likely to suffer from climatic cooling than high-elevation species/lineages. Late Pleistocene cooling appears to have had a rather positive effect on the population size of *E. v. roborowskii*. The neutrality tests and EBSP analysis identified signs of population expansion, and this process may contribute to the understanding of the low structure among populations of *E. v. roborowskii*. The date of rapid expansion is in accordance with an important climatic event (LGM) that is likely to have affected the population history of this lineage (Fig. 4). Disappearance of the Pleistocene lakes (Murzaev, 1966; Yang and Scuderi, 2010; Yang et al., 2011) and rapid desert expansion in the Turpan Depression during the Late Pleistocene (Bubenzer et al., 2016) may have favored the colonization of new sites and promoted the contact and gene flow among populations that were previously isolated. Furthermore, our ENM analyses mirrored that from genetic data in that the potential range of this lineage has increased within the Turpan Depression since the LGM (see Fig. 5). A plausible reason lays in the fact that a progressive drying of the climate in the Holocene and disappearance of the Pleistocene lakes in the Turpan Depression opened

space for the spread of the racerunners under suitable arid conditions. Surprisingly, our ENM results also suggest that most of the Junggar Depression where *E. v. velox* is currently distributed was a potentially suitable area for *E. v. roborowskii* during the LIG. However, it is unlikely that *E. v. roborowskii* colonized the Junggar Depression during the LIG because the Tianshan Mountains served as geographic barriers to dispersal (e.g., Cheng et al., 2017; Guo and Wang, 2007; Ludt et al., 2004). Moreover, compared to the range of *E. v. roborowskii* during the LIG, ENM analyses suggested expansions into the interior of the Turpan Depression during the LGM; this may have been facilitated by the desiccation of the mega-lake since *ca.* 30 ka (Yang et al., 2011). Hence, the current distribution of *E. v. roborowskii* is more similar to its LGM distribution than its LIG distribution, supporting *in situ* survival and expansion during the last glaciation. This scenario is apparently different from that predicted by the GM contraction model (Hewitt, 2004) but similar to that predicted by the GM expansion model (Galbreath et al., 2009).

4.4. Taxonomical implications

By increasing *E. velox* samples across its distribution range, we uncovered three more lineages than recognized by Liu et al. (2014). At present, the taxonomic situation of *E. velox* is far from being fully clarified. Because taxonomy reflects history, clarification is a prerequisite if we want to further study the evolutionary mechanisms accounting for the differentiation of the species. Traditionally, populations from Caucasus and adjacent western Kazakhstan were recognized as independent subspecies, *E. v. caucasia*, with differentiated morphological characteristics of dorsal patterns, pholidosis and body size as compared to the nominate form (Szczerbak, 1974, 1975). The type locality of this subspecies is located in Azerbaijan. In this study, we identified two well-differentiated clades with *p*-distances of 2.0% in 12S rRNA and 6.9% in cyt *b* gene (Table 1), corresponding to distinct geographic areas, i.e., Clade VII covering populations from Azerbaijan (area D) and Clade VI comprising populations from Ciscaucasia and adjacent western Kazakhstan (area E). Compared to other studies (Torstrom et al., 2014; and references therein), these genetic distances are similar to subspecies status. Furthermore, both BPP and bPTP analyses indicated that Clade VII represents a distinct genetic lineage. Although no apparent morphological differentiation between the populations from the two areas has been reported (Szczerbak, 1974, 1975), this divergence in *E. v. caucasia* sensu lato can be appreciated based on biogeography and mitochondrial DNA data. Thus, considering the type locality, we designate Clade VII as the traditionally recognized *E. v. caucasia* sensu stricto, while Clade VI may be assigned to an undescribed subspecies.

Populations of *E. velox* from Turkmenistan exhibit great morphological deviations compared to the nominate form (Szczerbak, 1974, 1975). In addition to populations from the Iranian Plateau, populations in Turkmenistan (Clade IV) harbor high genetic diversity (Table S9; Fig. S6) and substantial genetic differentiation from other clades (*p*-distance over 8.0% in cyt *b* gene) (see Table S6.2). Although the molecular basis required to recognize Turkmenistan Clade IV as a distinct genetic lineage is provided by this study, the integrative taxonomic approach (see Padial et al., 2010 for review) seems to be necessary to determine the species boundaries and determine the diagnostic morphological characteristics. This approach incorporates different sets of characteristics as separate lines of evidence (e.g., genetic, morphological, and ecological) and then uses each line of evidence when considering the taxonomic status of species/subspecies. Clade IX comprising populations from midwestern Kazakhstan showed modest divergence from *E. v. velox* (*p*-distance of 2.4% in cyt *b* gene between IX and X) and the Uzbekistan Clade VIII (*p*-distance of 1.1% in cyt *b* gene between VIII and IX). Both species delimitation analyses recognized the clades VIII and IX as distinct genetic lineages. In addition, Chirikova (2004) observed a clinal variations among *E. velox* populations from west to east in Kazakhstan. Thus, concerning the subspecies status of the Uzbekistan Clade VIII (Liu et al., 2014), we propose that Clade IX should be recognized as a separate subspecies.

We also clarify the taxonomic status of *E. v. roborowskii* from the Turpan Depression, northwest China. The male adults of this form have a dorsal pattern of irregular dark spots, and laterally rows of blue eye-like spots with bright dark-edge (see Fig. 2; Szczerbak, 2003; Zhao et al., 1999). Our recent morphological work also indicated apparent scalation deviations between *E. v. velox* and *E. v. roborowskii* (Chirikova et al., unpubl. data); the latter have significantly lower amounts of femoral pores and a higher percentage of specimens with one enlarged preanal scale (72.7%). Furthermore, *E. v. roborowskii* harbors high genetic differentiation from other clades (*p*-distance exceeding 10% in cyt *b* gene), and is delimitated as a distinct genetic lineage by both of BPP and bPTP analyses. Thus, taking multiple lines of evidence together, *E. v. roborowskii* deserves recognition at the species level under the general lineage concept of species (de Queiroz, 2007) and associated operational species-delimitation criteria (Wiens and Penkrot, 2002; Torstrom et al., 2014).

5. Concluding remarks

Our findings suggest that the intensified aridifications from the Late Pliocene onwards drove the diversification of *E. velox* in general, and particularly the “Out of Iranian Plateau” origin of the widespread *E. velox*, while geography and the Quaternary glaciations further shaped the evolution of this lizard. Specifically, the diversification between the Caucasus and Central Asia clades, and within the Central Asia clade may have been established and maintained in part by repeated transgressions of the Caspian Sea during the Pleistocene and Holocene. Our observations of the widespread *E. velox* likely underscore a general biogeographic/evolutionary process that has been operating on many other temperate organisms in ACA. Unlike in the high-latitude regions where Pleistocene glaciation cycles might have erased entire populations (Hewitt, 2004), in the western part of midlatitude Asian continent (i.e., ACA), many organisms may have more successfully adapted to various climatic stresses and were able to thrive during severe glacial periods because of the great ecological and geographic heterogeneity in the region. The effect of the Late Pleistocene climatic changes on the historical demography of arid-adapted species may be lineage-specific, depending predominantly on animal physiology and geography. We envisage that ACA served as crucial refugia during past environmental crises, and the vast dynamic areas with complex habitat diversity acted as important corridors for populations exchange, the generation of new lineages and species and fostered genetic diversity across the ACA. Further studies using the rigorous testing of hypotheses are likely to yield an understanding of the drivers of evolutionary change.

Acknowledgments

We are indebted to Tatjana Dujsebayeva and Marina Chirikova (Laboratory of Ornithology and Herpetology, Institute of Zoology, Kazakhstan) for providing many samples from Kazakhstan, and to Natalia Ananjeva (Zoological Institute, Russian Academy of Sciences) for providing three samples from Azerbaijan, and to Theodore J. Papenfuss (Museum of Vertebrate Zoology, University of California) for loaning three samples from Turkmenistan and Iran. We thank Feng Xu (Xinjiang Institute of Ecology and Geography, Chinese Academy of Sciences), Shujun Zhang, Tianhe Zhou, Dajiang Li, Xiong Gong, and Qi Song for assistance with fieldwork in Xinjiang Uygur Autonomous Region, China. We thank Tatjana Dujsebayeva for her valuable comments on an early version of this article. This article benefited greatly from insightful comments by the Editors and two anonymous reviewers.

Funding

This study was supported by the Strategic Priority Research Program of the Chinese Academy of Sciences (XDPA20050201), the National Natural Science Foundation of China (31672270, 31272281, 31560591, 31572240, 31872959), the Ministry of Science and Technology of the People's Republic of China (2015DFR30790), and the National Key Research and Development Program of China (2017YFC0505202).

Appendix A. Supplementary material

Supplementary data to this article can be found online at https://doi.org/10.1016/j.ympev.2018.10.029.

References

Abreu, V., Nummedal, D., 2007. Miocene to Quaternary sequence stratigraphy of the South and Central Caspian Basins. In: In: Yilmaz, P.O., Isaken, G.H. (Eds.), Oil and Gas of the Greater Capsian area, AAPG Studies in Geology 55. pp. 65–86.

Aljanabi, S.M., Martinez, I., 1997. Universal and rapid salt-extraction of high quality genomic DNA for PCR-based techniques. Nucl. Acids Res. 25, 4692–4693.

An, Z.S., Kutzbach, J.E., Prell, W.L., Porter, S.C., 2001. Evolution of Asian monsoons and phased uplift of the Himalaya-Tibetan plateau since Late Miocene times. Nature 411, 62–66.

Arnerup, J., Högberg, N., Thor, G., 2004. Phylogenetic analysis of multiple loci reveal the population structure within *Letharia* in the Caucasus and Morocco. Mycol. Res. 108, 311–316.

Atamuradov, K.I., 1994. Paleogeography of turkmenistan. In: Fet, V., Atamuradov, K.I. (Eds.), Biogeography and Ecology of Turkmenistan. Kluwer Academic Publishers, Dordrecht, Boston, London, pp. 49–64.

Aubekerov, B., Gorbunov, A., 1999. Quaternary permafrost and mountain glaciation in Kazakhstan. Permafrost Periglac. Process 10, 65–80.

Avise, J.C., 2000. Phylogeography: The History and Formation of Species. Harvard University Press.

Avise, J.C., 2012. Molecular Markers, Natural History and Evolution. Springer Science & Business Media.

Axen, G.J., Lam, P.S., Grove, M., Stockli, D.F., Hassanzadeh, J., 2001. Exhumation of the west-central Alborz Mountains, Iran, Caspian subsidence, and collision-related tectonics. Geology 29, 559–562.

Ballard, J.W.O., Whitlock, M.C., 2004. The incomplete natural history of mitochondria. Mol. Ecol. 13, 729–744.

Bandelt, H.J., Forster, P., Röhl, A., 1999. Median-joining networks for inferring intraspecific phylogenies. Mol. Biol. Evol. 16, 37–48.

Bosboom, R.E., Dupont-Nivet, G., Houben, A.J.P., Brinkhuis, H., Villa, G., Mandic, O., Stoica, M., Zachariasse, W.J., Guo, Z., Li, C., Krijgsman, W., 2011. Late Eocene sea retreat from the Tarim Basin (west China) and concomitant Asian paleoenvironmental change. Palaeogeogr. Palaeoclimatol. Palaeoecol. 299, 385–398.

Brandley, M.C., Guiher, T.J., Pyron, R.A., Winne, C.T., Burbrink, F.T., 2010. Does dispersal across an aquatic geographic barrier obscure phylogeographic structure in the diamond-backed watersnake (*Nerodia rhombifer*)? Mol. Phylogenet. Evol. 57, 552–560.

Brown, J.L., 2014. SDMtoolbox: a python-based GIS toolkit for landscape genetic, biogeographic and species distribution model analyses. Methods Ecol. Evol. 5, 694–700.

Bubenzer, O., Hecht, S., Li, C.S., Li, X., Li, Y., Schukraft, G., Mächtle, B., 2016. Late Pleistocene (MIS2) environmental changes and palaeoclimatic dynamics around Aiding Lake in the Turpan Basin, Xinjiang Province, NW-China. Zeitschrift für Geomorphol., Suppl. Issues 60, 5–27.

Byrne, M., Yeates, D.K., Joseph, L., Kearney, M., Bowler, J., Williams, M.A., Cooper, S., Donnellan, S.C., Keogh, J.S., Leys, R., Melville, J., Murphy, D.J., Porch, N., Wyrwoll, K.H., 2008. Birth of a biome: insights into the assembly and maintenance of the Australian arid zone biota. Mol. Ecol. 17, 4398–4417.

Carnaval, A.C., Hickerson, M.J., Haddad, C.F., Rodrigues, M.T., Moritz, C., 2009. Stability predicts genetic diversity in the Brazilian Atlantic forest hotspot. Science 323, 785–789.

Carranza, S., Arnold, E.N., 2012. A review of the geckos of the genus *Hemidactylus* (Squamata: Gekkonidae) from Oman based on morphology, mitochondrial and nuclear data, with descriptions of eight new species. Zootaxa 3378, 1–95.

Cheng, J., Lv, X., Xia, L., Ge, D., Zhang, Q., Lu, L., Yang, Q., 2017. Impact of orogeny and environmental change on genetic divergence and demographic history of *Dipus sagitta* (Dipodoidea, Dipodinae) since the Pliocene in inland East Asia. J. Mamm. Evol. https://doi.org/10.1007/s10914-017-9397-6.

Chirikova, M.A., 2004. Variability of *Eremias velox* Pallas, 1771 (Reptilia, Sauria) from Kazakhstan. Selevinia 24–34 (in Russian with English abstract).

Clark, P.U., Dyke, A.S., Shakun, J.D., Carlson, A.E., Clark, J., Wohlfarth, B., Mitrovica, J.X., Hostetler, S.W., Mccabe, A.M., 2009. Last Glacial Maximum. Science 325, 710–714.

Coyne, J.A., Orr, H.A., 2004. Speciation. Sinauer Associates Inc., Sunderland, MA.

de Queiroz, K., 2007. Species concepts and species delimitation. Syst. Biol. 56, 879–886.

Dolukhanov, P.M., Chepalyga, A.L., Lavrentiev, N.V., 2010. The Khvalynian transgressions and early human settlement in the Caspian basin. Quatern. Int. 225, 152–159.

Drummond, A.J., Suchard, M.A., Xie, D., Rambaut, A., 2012. Bayesian phylogenetics with BEAUti and the BEAST 1.7. Mol. Biol. Evol. 29, 1969–1973.

Dubey, S., Zaitsev, M., Cosson, J.F., Abdukadier, A., Vogel, P., 2006. Pliocene and Pleistocene diversification and multiple refugia in a Eurasian shrew (*Crocidura suaveolens* group). Mol. Phylogenet. Evol. 38, 635–647.

Eremchenko, V., Panfilov, A., 1999. Taxonomic position and geographic relations of a lacertid lizard *Eremias velox* from the Issyk-Kul lake depression, Tien Shan Mountains, Kyrgyzstan. Sci. New Tech. 99, 119–125 (in Russian with English abstract).

Excoffier, L., Lischer, H.E., 2010. Arlequin suite ver 3.5: a new series of programs to perform population genetics analyses under Linux and Windows. Mol. Ecol. Resour. 10, 564–567.

Excoffier, L., Smouse, P.E., Quattro, J.M., 1992. Analysis of molecular variance inferred from metric distances among DNA haplotypes, application to human mitochondrial DNA restriction data. Genetics 131, 479–491.

Fang, X., Lü, L., Yang, S., Li, J., An, Z., Jiang, P., Chen, X., 2002. Loess in Kunlun Mountains and its implications on desert development and Tibetan Plateau uplift in west China. Sci. China, Ser. D 45, 289–299.

Felsenstein, J., 1985. Confidence limits on phylogenies: an approach using the bootstrap. Evolution 39, 783–791.

Forte, A.M., Cowgill, E., 2013. Late Cenozoic base-level variations of the Caspian Sea: a review of its history and proposed driving mechanisms. Palaeogeogr. Palaeoclimatol. Palaeoecol. 386, 392–407.

Fu, Y.X., 1997. Statistical tests of neutrality of mutations against population growth, hitchhiking and background selection. Genetics 147, 915–925.

Galbreath, K.E., Hafner, D.J., Zamudio, K.R., 2009. When cold is better: climate-driven elevation shifts yield complex patterns of diversification and demography in an alpine specialist (American pika, *Ochotona princeps*). Evolution 63, 2848–2863.

Galtier, N., Nabholz, B., Glémin, S., Hurst, G.D.D., 2009. Mitochondrial DNA as a marker of molecular diversity: a reappraisal. Mol. Ecol. 18, 4541–4550.

Garcia-Porta, J., Litvinchuk, S.N., Crochet, P.A., Romano, A., Geniez, P.H., Lo-Valvo, M., Lymberakis, P., Carranza, S., 2012. Molecular phylogenetics and historical biogeography of the west-palearctic common toads (*Bufo bufo* species complex). Mol. Phylogenet. Evol. 63, 113–130.

Grassi, F., Mattia, F.D., Zecca, G., Sala, F., Labra, M., 2008. Historical isolation and Quaternary range expansion of divergent lineages in wild grapevine. Biol. J. Linn. Soc. 95, 611–619.

Green, T., Abdullayev, N., Hossack, J., Riley, G., Roberts, A.M., 2009. Sedimentation and subsidence in the South Caspian Basin. Azerbaijan. Geol. Soc. Spec. Publ. 312, 241–260.

Guo, X., Dai, X., Chen, D., Papenfuss, T.J., Ananjeva, N.B., Melnikov, D.A., Wang, Y., 2011. Phylogeny and divergence times of some racerunner lizards (Lacertidae: *Eremias*) inferred from mitochondrial 16S rRNA gene segments. Mol. Phylogenet. Evol. 61, 400–412.

Guo, X., Wang, Y., 2007. Partitioned Bayesian analyses, dispersal-vicariance analysis, and the biogeography of Chinese toad-headed lizards (Agamidae: *Phrynocephalus*): a re-evaluation. Mol. Phylogenet. Evol. 45, 643–662.

Guo, Z.T., Ruddiman, W.F., Hao, Q.Z., Wu, H.B., Qiao, Y.S., Zhu, R.X., Peng, S.Z., Wei, J.J., Yuan, B.Y., Liu, T.S., 2002. Onset of Asian desertification by 22 Myr ago inferred from loess deposits in China. Nature 416, 159–163.

Guo, Z.T., Sun, B., Zhang, Z.S., Peng, S.Z., Xiao, G.Q., Ge, J.Y., Hao, Q.Z., Qiao, Y.S., Liang, M.Y., Liu, J.F., Yin, Q.Z., Wei, J., 2008. A major reorganization of Asian climate by the early Miocene. Clim. Past 4, 153–174.

Hewitt, G.M., 1996. Some genetic consequences of ice ages, and their role in divergence and speciation. Biol. J. Linn. Soc. 58, 247–276.

Hewitt, G.M., 2000. The genetic legacy of the Quaternary ice ages. Nature 405, 907–913.

Hewitt, G.M., 2004. Genetic consequences of climatic oscillations in the Quaternary. Philos. Trans. R. Soc. Lond. B 359, 183–195.

Hijmans, R.J., Cameron, S.E., Parra, J.L., Jones, P.G., Jarvis, A., 2005. Very high resolution interpolated climate surfaces for global land areas. Int. J. Climatol. 25, 1965–1978.

Jia, D.R., Abbott, R.J., Liu, T.L., Mao, K.S., Bartish, I.V., Liu, J.Q., 2012. Out of the Qinghai-Tibet Plateau: evidence for the origin and dispersal of Eurasian temperate plants from a phylogeographic study of *Hippophae rhamnoides* (Elaeagnaceae). New Phytol. 194, 1123–1133.

Jones, R.W., Simmons, M., 1996. A review of the stratigraphy of Eastern Paratethys (Oligocene–Holocene). Bull. Nat. Hist. Mus. Geol. 52, 25–49.

Kass, R.E., Raftery, A.E., 1995. Bayes factors. J. Am. Stat. Assoc. 90, 773–795.

Kearns, A.M., Joseph, L., Toon, A., Cook, L.G., 2014. Australia's arid-adapted butcherbirds experienced range expansions during Pleistocene glacial maxima. Nat. Commun. 5, 3994.

Kumar, S., Stecher, G., Tamura, K., 2016. MEGA7: molecular evolutionary genetics analysis version 7.0 for bigger datasets. Mol. Biol. Evol. 33, 1870–1874.

Lanfear, R., Calcott, B., Ho, S.Y., Guindon, S., 2012. Partitionfinder: combined selection of partitioning schemes and substitution models for phylogenetic analyses. Mol. Biol. Evol. 29, 1695–1701.

Larkin, M.A., Blackshields, G., Brown, N.P., Chenna, R., McGettigan, P.A., McWilliam, H., Valentin, F., Wallace, I.M., Wilm, A., Lopez, R., Thompson, J.D., Gibson, T.J., Higgins, D.G., 2007. Clustal W and Clustal X version 2.0. Bioinformatics 23, 2947–2948.

Leaché, A.D., Fujita, M.K., 2010. Bayesian species delimitation in West African forest geckos (*Hemidactylus fasciatus*). Proc. Roy. Soc. Lond. Ser. B Biol. Sci. 277, 3071–3077.

Librado, P., Rozas, J., 2009. DnaSP v5: a software for comprehensive analysis of DNA polymorphism data. Bioinformatics 25, 1451–1452.

Liu, J., Ananjeva, N.A., Chirikova, M.A., Milto, K.D., Guo, X., 2014. Molecular assessment and taxonomic status of the rapid racerunner (*Eremias velox* complex) with particular attention to the populations in Northwestern China. Asian Herpetol. Res. 5, 12–25.
Lu, H., Wang, X., Li, L., 2010. Aeolian sediment evidence that global cooling has driven late Cenozoic stepwise aridification in central Asia. Geol. Soc. Spec. Publ. 342, 29–44.
Lu, H., Yi, S., Xu, Z., Zhou, Y., Zeng, L., Zhu, F., Feng, H., Dong, L., Zhuo, H., Yu, K., Mason, J., Wang, X., Chen, Y., Lu, Q., Wu, B., Dong, Z., Qu, J., Wang, X., Guo, Z., 2013. Chinese deserts and sand fields in Last Glacial Maximum and Holocene Optimum. Chin. Sci. Bull. 58, 2775–2783.
Ludt, C.J., Schroeder, W., Rottmann, O., Kuehn, R., 2004. Mitochondrial DNA phylogeography of red deer (*Cervus elaphus*). Mol. Phylogenet. Evol. 31, 1064–1083.
Lv, X., Xia, L., Ge, D., Wen, Z., Qu, Y., Lu, L., Yang, Q., 2016. Continental refugium in the Mongolian Plateau during Quaternary glacial oscillations: phylogeography and niche modelling of the endemic desert hamster, *Phodopus roborovskii*. PLoS One 11, e0148182.
Mamedov, A.V., 1997. The late Pleistocene-Holocene history of the Caspian Sea. Quatern. Int. 41–42, 161–166.
Manceau, V., Despres, L., Bouvet, J., Taberlet, P., 1999. Systematics of the genus *Capra* inferred from mitochondrial DNA sequence data. Mol. Phylogenet. Evol. 13, 504–510.
Melville, J., Hale, J., Mantziou, G., Ananjeva, N.B., Milto, K., Clemann, N., 2009. Historical biogeography, phylogenetic relationships and intraspecific diversity of agamid lizards in the Central Asian deserts of Kazakhstan and Uzbekistan. Mol. Phylogenet. Evol. 53, 99–112.
Miao, Y., Herrmann, M., Wu, F., Yan, X., Yang, S., 2012. What controlled Mid-Late Miocene long-term aridification in Central Asia? – Global cooling or Tibetan Plateau uplift: a review. Earth Sci. Rev. 112, 155–172.
Mosar, J., Kangarli, T., Bochud, M., Glasmacher, U.A., Rast, A., Brunet, M.-F., Sosson, M., 2010. Cenozoic-Recent tectonics and uplift in the Greater Caucasus: a perspective from Azerbaijan. Geol. Soc. Spec. Publ. 340, 261–280.
Murzaev, E.M., 1966. The Nature of Xinjiang and Formation of the Deserts in Central Asia. Science Press, Moscow (in Russian).
Myers, N., Mittermeier, R.A., Mittermeier, C.G., Da Fonseca, G.A., Kent, J., 2000. Biodiversity hotspots for conservation priorities. Nature 403, 853–858.
Neiber, M.T., Hausdorf, B., 2015. Phylogeography of the land snail genus *Circassina* (Gastropoda: Hygromiidae) implies multiple Pleistocene refugia in the western Caucasus region. Mol. Phylogenet. Evol. 93, 129–142.
Newman, C.E., Austin, C.C., 2015. Thriving in the cold: glacial expansion and post-glacial contraction of a temperate terrestrial salamander (*Plethodon serratus*). PLoS One 10, e0130131.
Padial, J.M., Miralles, A., De la Riva, I., Vences, M., 2010. The integrative future of taxonomy. Front. Zool. 7, 16.
Pavlicev, M., Mayer, W., 2009. Fast radiation of the subfamily Lacertinae (Reptilia: Lacertidae): history or methodical artefact? Mol. Phylogenet. Evol. 52, 727–734.
Peterson, A.T., Soberón, J., Sánchez-Cordero, V., 1999. Conservatism of ecological niches in evolutionary time. Science 285, 1265–1267.
Phillips, S.J., Anderson, R.P., Schapire, R.E., 2006. Maximum entropy modeling of species geographic distributions. Ecol. Model. 190, 231–259.
Phillips, S.J., Dudík, M., 2008. Modeling of species distributions with Maxent: new extensions and a comprehensive evaluation. Ecography 31, 161–175.
Popov, S.V., Antipov, M.P., Zastroshnov, A.S., Kurina, E.E., Pinchuk, T.N., 2010. Sea-level fluctuations on the northern shelf of the eastern Paratethys in the Oligocene-Neogene. Stratigr. Geo. Correl. 18, 200–224.
Provan, J., Bennett, K.D., 2008. Phylogeographic insights into cryptic glacial refugia. Trends Ecol. Evol. 23, 564–571.
Ramos-Onsins, S.E., Rozas, J., 2002. Statistical properties of new neutrality tests against population growth. Mol. Biol. Evol. 19, 2092–2100.
Rastegar-Pouyani, E.R., 2009. The phylogeny of the *Eremias velox* complex of the Iranian Plateau and Central Asia (Reptilia, Lacertidae): molecular evidence from ISSR-PCR fingerprints. Iran. J. Animal Biosystemat. 5, 33–46.
Rastegar-Pouyani, E.R., Noureini, S.K., Rastegar-Pouyani, N.R., Joger, U., Wink, M., 2012. Molecular phylogeny and intraspecific differentiation of the *Eremias velox* complex of the Iranian Plateau and Central Asia (Sauria, Lacertidae). J. Zool. Systemat. Evol. Res. 50, 220–229.
Raymo, M.E., 1994. The initiation of Northern Hemisphere glaciation. Annu. Rev. Earth Planet. Sci. 22, 353–383.
Ritchie, A.M., Lo, N., Ho, S.Y.W., 2017. The impact of the tree prior on molecular dating of data sets containing a mixture of inter- and intraspecies sampling. Syst. Biol. 66, 413–425.
Ronquist, F., Teslenko, M., van der Mark, P., Ayres, D.L., Darling, A., Hohna, S., Larget, B., Liu, L., Suchard, M.A., Huelsenbeck, J.P., 2012. MrBayes 3.2: efficient Bayesian phylogenetic inference and model choice across a large model space. Syst. Biol. 61, 539–542.
Ryan, W.B.F., Major, C.O., Lericolais, G., Goldstein, S.L., 2003. Catastrophic flooding of the Black Sea. Annu. Rev. Earth Planet Sci. 31, 525–554.
Rychagov, G.I., 1997. Holocene oscillations of the Caspian Sea, and forecasts based on palaeogeographical reconstructions. Quatern. Int. 41, 167–172.
Sanmartín, I., 2003. Dispersal vs. vicariance in the Mediterranean: historical biogeography of the Palearctic Pachydeminae (Coleoptera, Scarabaeoidea). J. Biogeogr. 30, 1883–1897.
Schoener, T.W., 1968. The *Anolis* lizards of Bimini: resource partitioning in a complex fauna. Ecology 49, 704–726.
Seddon, J.M., Santucci, F., Reeve, N., Hewitt, G.M., 2002. Caucasus Mountains divide postulated postglacial colonization routes in the white-breasted hedgehog, *Erinaceus concolor*. J. Evol. Biol. 15, 463–467.
Shabanian, E., Siame, L., Bellier, O., Benedetti, L., Abbassi, M.R., 2009. Quaternary slip rates along the northeastern boundary of the Arabia-Eurasia collision zone (Kopeh Dagh Mountains, Northeast Iran). Geophys. J. Int. 178, 1055–1077.
Shi, C.M., Ji, Y.J., Liu, L., Wang, L., Zhang, D.X., 2013. Impact of climate changes from Middle Miocene onwards on evolutionary diversification in Eurasia: insights from the mesobuthid scorpions. Mol. Ecol. 22, 1700–1716.
Shi, Y.F., Cui, Z.J., Su, Z., 2006. The Quaternary Glaciations and Environmental Variations in China. Hebei Science and Technology Press, Shijiazhuang, China (in Chinese).
Sindaco, R., Jeremcěnko, V.K., 2008. The Reptiles of the Western Palearctic. 1. Annotated Checklist and Distributional Atlas of the Turtles, Crocodiles, Amphisbaenians and Lizards of Europe, North Africa, Middle East and Central Asia. Latina, Edizioni Belvedere, Italy.
Sorokin, V.M., 2011. Correlation of Upper Quaternary deposits and paleogeography of the Black and Caspian seas. Stratigr. Geol. Correl. 19, 563–578.
Stamatakis, A., 2014. RAxML version 8: a tool for phylogenetic analysis and post-analysis of large phylogenies. Bioinformatics 30, 1312–1313.
Steiniger, F.F., Rögl, F., 1984. Paleogeography and palinspastic reconstruction of the Neogene of the Mediterranean and Paratethys. Geol. Soc. Spec. Publ. 17, 659–668.
Sun, J., Ye, J., Wu, W., Ni, X., Bi, S., Zhang, Z., Liu, W., Meng, J., 2010. Late Oligocene-Miocene mid-latitude aridification and wind patterns in the Asian interior. Geology 38, 515–518.
Synes, N.W., Osborne, P.E., 2011. Choice of predictor variables as a source of uncertainty in continental-scale species distribution modelling under climate change. Global Ecol. Biogeogr. 20, 904–914.
Szczerbak, N.N., 1974. Yashchurki Palearktiki (The Palearctic Racerunners). Naukova Dumka Press, Kiev (in Russian).
Szczerbak, N.N., 1975. Geographical variability and intraspecies taxonomy of *Eremias velox* Pall., 1771 (Reptilia, Sauria). Vestnik Zool. 6, 24–33 (in Russian with English abstract).
Szczerbak, N.N., 2003. Guide to the Reptiles of the Eastern Palearctic. Krieger Publishing Company, Malabar, Florida.
Tajima, F., 1989. Statistical method for testing the neutral mutation hypothesis by DNA polymorphism. Genetics 123, 585–595.
Tamar, K., Carranza, S., Sindaco, R., Moravec, J., Trape, J.F., Meiri, S., 2016. Out of Africa: phylogeny and biogeography of the widespread genus *Acanthodactylus* (Reptilia: Lacertidae). Mol. Phylogenet. Evol. 103, 6–18.
Tang, Z., Ding, Z., White, P.D., Dong, X., Ji, J., Jiang, H., Luo, P., Wang, X., 2011. Late Cenozoic central Asian drying inferred from a palynological record from the northern Tian Shan. Earth Planet. Sci. Lett. 302, 439–447.
Tarkhnishvili, D., Hille, A., Böhme, W., 2001. Humid forest refugia, speciation and secondary introgression between evolutionary lineages: differentiation in a Near Eastern brown frog, *Rana maerocnemis*. Biol. J. Linn. Soc. 74, 141–156.
Tarkhnishvili, D.N., Thorpe, R.S., Arntzen, J.W., 2000. Pre-Pleistocene refugia and differentiation between populations of the Caucasian salamander (*Mertensiella caucasica*). Mol. Phylogenet. Evol. 14, 414–422.
Tews, J., Brose, U., Grimm, V., Tielbörger, K., Wichmann, M.C., Schwager, M., Jeltsch, F., 2004. Animal species diversity driven by habitat heterogeneity/diversity: the importance of keystone structures. J. Biogeogr. 31, 79–92.
Torstrom, S.M., Pangle, K.L., Swanson, B.J., 2014. Shedding subspecies: the influence of genetics on reptile subspecies taxonomy. Mol. Phylogenet. Evol. 76, 134–143.
Trifonov, V.G., Ivanova, T.P., Bachmanov, D.M., 2012. Recent mountain building of the central Alpine-Himalayan Belt. Geotectonics 46, 315–332.
Tseng, S.P., Li, S.H., Hsieh, C.H., Wang, H.Y., Lin, S.M., 2014. Influence of gene flow on divergence dating – implications for the speciation history of *Takydromus* grass lizards. Mol. Ecol. 23, 4770–4784.
Tudryn, A., Chalié, F., Lavrushin, Y.A., Antipov, M.P., Spiridonova, E.A., Lavrushin, V., Tucholka, P., Leroy, S.A.G., 2013. Late Quaternary Caspian Sea environment: Late Khazarian and Early Khvalynian transgressions from the lower reaches of the Volga River. Quatern. Int. 292, 193–204.
Väinölä, R., Vainio, J.K., Palo, J.U., 2001. Phylogeography of “glacial relict” *Gammaracanthus* (Crustacea, Amphipoda) from boreal lakes and the Caspian and White seas. Can. J. Fish. Aquat. Sci. 58, 2247–2257.
Vandenberghe, J., French, H.M., Gorbunov, A., Marchenko, S., Velichko, A.A., Jin, H., Cui, Z., Zhang, T., Wan, X., 2014. The Last Permafrost Maximum (LPM) map of the Northern Hemisphere: permafrost extent and mean annual air temperatures, 25–17 ka BP. Boreas 43, 652–666.
Wang, Y., Autumn, K., 1990. Home range size and spatial distribution of *Phrynocephalus przewalskii*, *P. axillaris* and *Eremias velox*. In: Zhao, E.M. (Ed.), From Water onto Land – A Volume Issued to Commemorate the 90th Birthday of the Late Professor Liu Cheng-Zhao. China Forestry Publishing House, Beijing, pp. 125–132 (in Chinese with English abstract).
Wang, I.J., Bradburd, G.S., 2014. Isolation by environment. Mol. Ecol. 23, 5649–5662.
Wang, L., Ji, J., Sun, D., Xu, Q., Han, B., 2015. Chronological constraints on multi-staged rapid cooling of the Tianshan Mountains inferred from apatite fission track analysis of modern river sands. Sci. Chin. Earth Sci. 58, 1305–1319.
Wang, Y., Zhao, L.M., Fang, F.J., Liao, J.C., Liu, N.F., 2013. Intraspecific molecular phylogeny and phylogeography of the *Meriones meridianus* (Rodentia: Cricetidae) complex in northern China reflect the processes of desertification and the Tianshan Mountains uplift. Biol. J. Linn. Soc. 110, 362–383.
Warren, D.L., Glor, R.E., Turelli, M., 2008. Environmental niche equivalency versus conservatism: quantitative approaches to niche evolution. Evolution 62, 2868–2883.
Warren, D.L., Glor, R.E., Turelli, M., 2010. ENMTools: a toolbox for comparative studies of environmental niche models. Ecography 33, 607–611.
Wiens, J.J., Graham, C.H., 2005. Niche conservatism: integrating evolution, ecology, and conservation biology. Annu. Rev. Ecol. Evol. Syst. 36, 519–539.
Wiens, J.J., Penkrot, T.A., 2002. Delimiting species using DNA and morphological

variation and discordant species limits in spiny lizards (*Sceloporus*). Syst. Biol. 51, 69–91.
Wisz, M.S., Hijmans, R.J., Li, J., Peterson, A.T., Graham, C.H., Guisan, A., 2008. Effects of sample size on the performance of species distribution models. Divers. Distrib. 14, 763–773.
Yang, X., Preusser, F., Radtke, U., 2006. Late Quaternary environmental changes in the Taklamakan Desert, western China, inferred from OSL-dated lacustrine and aeolian deposits. Quatern. Sci. Rev. 25, 923–932.
Yang, X., Scuderi, L.A., 2010. Hydrological and climatic changes in deserts of China since the late Pleistocene. Quatern. Res. 73, 1–9.
Yang, X., Scuderi, L.A., Paillou, P., Liu, Z., Li, H., Ren, X., 2011. Quaternary environmental changes in the drylands of China – a critical review. Quatern. Sci. Rev. 30, 3219–3233.
Yang, Z., Rannala, B., 2010. Bayesian species delimitation using multilocus sequence data. Proc. Natl. Acad. Sci. USA 107, 9264–9269.
Yang, Z., Rannala, B., 2014. Unguided species delimitation using DNA sequence data from multiple loci. Mol. Biol. Evol. 31, 3125–3135.
Yu, Y., Harris, A.J., Blair, C., He, X., 2015. RASP (Reconstruct Ancestral State in Phylogenies): a tool for historical biogeography. Mol. Phylogenet. Evol. 87, 46–49.
Zhang, J., Kapli, P., Pavlidis, P., Stamatakis, A., 2013. A general species delimitation method with applications to phylogenetic placements. Bioinformatics 29, 2869–2876.
Zhang, Z.S., Wang, H.J., Guo, Z.T., Jiang, D.B., 2007. What triggers the transition of palaeoenvironmental patterns in China, the Tibetan Plateau uplift or the Paratethys Sea retreat? Palaeogeogr. Palaeoclimatol. Palaeoecol. 245, 317–331.
Zhao, E.M., Zhao, K.T., Zhou, K.Y., 1999. Fauna Sinica, Reptilia (Squamata: Lacertilia), vol. 2 Science Press, Beijing (in Chinese).
Zinenko, O., Stümpel, N., Mazanaeva, L., Bakiev, A., Shiryaev, K., Pavlov, A., Kotenko, T., Kukushkin, O., Chikin, Y., Duisebayeva, T., Nilson, G., Orlov, N.L., Tuniyev, S., Ananjeva, N.B., Murphy, R.W., Joger, U., 2015. Mitochondrial phylogeny shows multiple independent ecological transitions and northern dispersion despite of Pleistocene glaciations in meadow and steppe vipers (*Vipera ursinii and Vipera renardi*). Mol. Phylogenet. Evol. 84, 85–100.
Zubakov, V.A., 2001. History and causes of variations in the Caspian Sea level: the Miopliocene, 7.1–1.95 million years ago. Water Resour. 28, 249–256.